Title
Investigating of the interplay between primary structure and conformation of the [PSI+] prion protein by systematic analysis of the prion propagation cycle

Author
Verges, Katherine Joanne

Publication Date
2009

Peer reviewed|Thesis/dissertation

Investigating of the interplay between primary structure and conformation of the [*PSI*$^{+}$] prion protein by systematic analysis of the prion propagation cycle

by

Katherine J. Verges

DISSERTATION

Submitted in partial satisfaction of the requirements for the degree of

DOCTOR OF PHILOSOPHY

in

BIOCHEMISTRY

in the

GRADUATE DIVSION

of the

UNIVERSITY OF CALIFORNIA, SAN FRANCISCO

This work is dedicated to Mrs. Josephine Filaski.

ACKNOWLEDGEMENTS

Jonathan

First and foremost, I would like to thank Jonathan, who is a very giving and patient mentor. Jonathan's insight and foresight set him apart as an extraordinary scientist. His good nature sets him apart as an admirable person. I learned a lot from Jonathan, and I am grateful to have worked with him.

Thesis Committee

Carol Gross, Dyche Mullins, and Geeta Narlikar composed an extremely supportive committee. Their scientific suggestions and feedback were crucial to the success of my project, and their encouragement on a more personal level was critical for my development during graduate school.

The Weissman Lab

Thanks to all the exceptional people in the Weissman lab, and especially those belonging to the [*PSI*$^{+}$] side. Sean Collins, my friend, rotation advisor, and subsequent colleague, is a superb scientist and amiable person. Kim Tipton, who worked closely with me, gave me much scientific advice. Clement Chu has fixed the many things that I broke while in lab, and for that I will be eternally grateful. Dale Cameron was always an enjoyable and well-grounded colleague who provided essential perspective. Brandon Toyama is an exceptional scientist and dear friend; I have learned a tremendous amount while working with Brandon, and his help has been instrumental in the success of my project. Cat Foo,

the most recent addition to the [*PSI*$^{+}$] group, has been a wonderful colleague, and it has been a joy to work with Cat.

My Family

Chris is a wonderfully encouraging spouse. Without his backing, my graduate career would have approached the impossible and, at the least, would have been much less enjoyable.

My parents have redefined unconditional love. Thank you very much for everything you've done for me and for always encouraging me, even when opportunities brought me far from home.

Classmates

Claire Rowe has been an invaluable source of encouragement. Without Claire, I would have never made it through graduate school while keeping my sanity. Claire has helped me through so many challenges, and I will always appreciate her guidance. Erin Toyama provided answers to my endless questions, aided my experimentation, and became a great friend. I appreciate Erin's help, both scientific and personal. All of my classmates have provided a supportive network to which I have turned time and time again. They are all exceptional scientists and wonderful people, and I know they will all go on to succeed.

Manny, Alice, Sue, and Danny

Manny is in many ways the backbone of the Weissman lab who keeps it functioning. He is very giving and has helped me immensely. Alice has been a wonderful source of organization in our chaotic lab, and I have greatly enjoyed our conversations. Sue and Danny have kept the graduate program alive with their support and dedication.

CONTRIBUTIONS

Jonathan Weissman and Kim Tipton provided crucial guidance on the creation and execution of these projects. Peter Chien and the Tania Baker lab provided the reagents, protocols, and advice that were essential for my pursuing the Clp project. Motomassa Tanaka created many of the assays used to characterize fibers *in vitro*, and provided helpful advice for performing them. Brandon Toyama developed the H/X NMR protocols, in addition to acquiring and analyzing the NMR data presented in this work.

Investigating of the interplay between primary structure and conformation of the [*PSI*$^+$] prion protein by systematic analysis of the prion propagation cycle

Katherine J. Verges

Abstract

Prions, or infectious proteins, are self-templating ordered aggregates capable of replication. One such prion, [*PSI*$^+$], is caused by the aggregation of the translation termination factor Sup35 in *Saccharomyces cerevisiae*. Although much more amenable to experimentation, yeast prions share many characteristics with their mammalian counterparts, including the existence of prion strain variants and the ability of single amino acids to modulate prion phenotypes in a manner that's specific to a particular prion strain variant. Yeast prions propagate through a cycle that consists of prion growth, division, and partitioning to daughter cells. Chapter 2 describes investigation of how single amino acid changes affect the ability of prions to propagate, through systematically probing each step of the prion propagation cycle. This work emphasizes partitioning as a crucial step in the prion replication cycle, highlighting it as an interesting area of future study. Chapter 3 describes an attempt to create a robust *in vitro* system to investigate how chaperones can act as molecular motors to divide extraordinarily stable prion particles. Unfortunately, this synthetic system was ultimately unable to divide prions *in vitro*.

TABLE OF CONTENTS

LIST OF FIGURES

CHAPTER 1

Introduction

Prions

Infectious proteins, termed prions, are self-templating proteinacious fibers capable of replication[1]. Prions represent an important and interesting subject of study, as their ability to innately form highly stable ordered aggregates presents intriguing protein folding and structural questions. Moreover, prions, in addition to other members of the larger class of amyloid-forming proteins, are highly associated with neurological diseases.

Amyloid-forming proteins can polymerize into self-templating fibers competent to recruit soluble protein and convert it to the amyloid form[1,2]. Amyloid fibers are highly stable, as they are resistant to heat and chemical denaturation[3]. Although there is variance in amyloid structure, amyloid-forming proteins all contain at least one domain capable of forming highly stable interactions between subunits composing the characteristic β-sheet rich amyloid core. While the precise mechanism of toxicity is yet to be determined, amyloid fibers are highly associated with a number of neurological diseases including Alzheimer's disease, Parkinson's disease, Huntington's disease, and Amyotrophic Lateral Sclerosis.

While all amyloid forming proteins form self-templating ordered aggregates, infectious amyloids (prions) have the additional, distinguishing characteristic of transmissibility. Notable examples are the transmissible spongiform encephalopathies (TSEs), which include Cruetzfeldt-Jakob disease in humans, bovine spongiform encephalopathy (BSE) in cattle, scrapie in sheep and goats, and chronic wasting disease (CWD) in deer and elk[4]. Variant Creutzfeldt-Jakob disease (*v*CJD) garnered heightened attention, as it may represent a new variant of BSE that is capable of crossing the species

barrier from bovine to humans and leads to a debilitating and fatal disease[5,6]. Sensitive to protease treatment and insensitive to nuclease digestion, the infectious material of the TSE's was suggested to be proteinaceous in nature, leading to "the protein-only hypothesis". Indeed, the causative agent in all of these diseases is a genomically encoded protein (PrP^{C}) that misfolds into an infectious form (PrP^{Sc})[1,7].

Prion strain variants

One of the most striking phenomenon in prion biology is the existence of prion strain variants, observed as varied disease phenotypes resulting from the misfolding of the same protein[4,8]. Originally, this phenotypic variance seemed to oppose the idea that a single protein could comprise the sole infectious agent of the TSEs. We now know that the same protein can fold into a range of different amyloid conformations, which can lead to different disease phenotypes[4,9]. Although observed in several species, two specific examples of prion strain variants include the drowsy and scratchy scrapie strains in sheep. Even though both phenotypes result from misfolding of the same protein, they vary greatly in their disease manifestations, as one is characterized by drowsiness and the other by scratchiness. Indeed, different prion strain variants can result in varied phenotypic expression, incubation time, and/or histological characteristics[4].

In addition to the observation of prion strain variants, it was also noted that specific single amino acid changes within the primary structure of the prion protein can modulate prion characteristics strain-specifically. Small changes to primary structure affect which prion strain variants are able to propagate, as well as influence the incubation time and other disease characteristics[4,10-12]. This phenomenon is especially

interesting in the context CJD, the human neurological disorder caused by misfolding of PrP. Humans have a naturally occurring methionine/valine polymorphism at position 129, and the genotype of an individual at this location (homozygous methionine, homozygous valine, or heterozygous) modulates characteristics of the disease phenotype of sporadic CJD (sCJD)[4,12]. In addition, the identity of this amino acid correlates with susceptibility of *v*CJD, the form of CJD caused by transmission of PrP fibers from bovine, as the presence of even a single valine may be completely protective against developing *v*CJD[13]. While it is speculated that specific amino acids can affect the structure of amyloids or modulate interactions with other cellular components, very little is known about how small changes in primary sequence can affect the ability of prion strain variants to propagate. These unknowns motivated the work described in chapter 3.

The yeast prion [*PSI*$^+$]

Although originally studied in mammals, prions have since been found to underlie a number of epigenetic phenomena in yeast. One such prion, [*PSI*$^+$], results from the aggregation of the translation termination factor Sup35 into amyloid fibers that are stably inherited. Studying the yeast prion [*PSI*$^+$] has several advantages over experimenting with mammalian prions including a short growth time, facile genetics, greater safety, and the existence of a relatively fast color read out of prion status. The [*PSI*$^+$] prion phenotype can be readily assessed through a red/white color readout resulting form Sup35 inactivation that causes nonsense suppression of an *ade1* reporter gene. Yeast that do not contain the prion appear red ([*psi*$^-$]), while those that do appear pink to white ([*PSI*$^+$]). Similar to their mammalian counterparts, yeast prions exhibit a range of strain

variants, revealed as varied degrees of nonsense suppression yielding an assortment of color phenotypes ranging from pink to white.

The [*PSI*$^{+}$] prion is stably inherited through a propagation cycle that includes fiber growth, division, and distribution to daughter cells. Fiber growth is thought to be an intrinsic property of amyloid-forming proteins, as a fragment of Sup35 containing its N-terminal and middle domains (SupNM) can spontaneously for fibers *in vitro*[14,15]. Fiber division rates are thought to depend on both the ability of a fiber to interact with host chaperone machinery and the structure of the fiber. Since molecular chaperones carry out fiber division *in vivo*, interactions with this machinery are essential for division[16,17]. Fiber structure modulates fiber stability, as structures with larger amyloid cores are more resistant to thermal denaturation and mechanical shearing[18,19]. Furthermore, decreased fiber stability is correlated with an increased division rate *in vivo*[18], presumably due to an increased rate of reaction with the chaperone machinery. Nevertheless, increased fiber division leads to an increase in the rate of generation of free fiber ends and tends to strengthen the prion phenotype. Although fiber growth and division have been extensively studied, little is known about prion partitioning. Despite its lack of attention, distribution of prion particles to daughter cells is a crucial step in the propagation process. Indeed, the work described in chapter 3 highlights the importance of this step.

One of the great strengths of the yeast system is the ability to study the same prion conformation both *in vitro* and *in vivo*. One can purify the prion forming domain of Sup35 (SupNM) recombinantly expressed in *E. coli*, form fibers *in vitro*, and introduce these fibers into yeast via a fiber infection protocol[9,20]. Indeed, infection with *in vitro* formed fibers is sufficient to convert yeast from [*psi*$^{-}$] to [*PSI*$^{+}$]. Moreover, fibers formed

in vitro at different temperatures (4˚C or 37˚C) give rise to characteristic and different *in vivo* phenotypes (white or pink, respectively)[9]. Further structural studies have shown that the varied phenotypes result from different conformations of the underlying amyloid structure[18,19]. The first 40 amino acids of the Sup35 sequence comprise the amyloid core of Sc4 fibers (formed at 4˚C). In Sc37 fibers (formed at 37˚C), this region is nearly doubled to encompass the first 70 amino acids. Additionally, Sc4 fibers are more fragile *in vitro* and replicate more quickly *in vivo*. Thus, a smaller amyloid core is associated with more fragile fibers and a faster division rate *in vivo*. These studies have led to a quantitative model in which prion phenotype strengthens with increased division and growth rates[18].

While the growth rate and stability of [*PSI*$^{+}$] fibers appear to be intrinsic properties of Sup35 and the conformations it can adopt, their *in vivo* division requires the cellular chaperone machinery[16,17]. In particular, the AAA+ ATPase Hsp104 acts in concert with Hsp70 (Ssa1) and Hsp40 (Sis1) to sever prion particles *in vivo*[16,21-23]. This process is thought to occur by extraction of Sup35 monomers from fibers and translocation of these monomers through the central pore of Hsp104. Three *E coli* AAA+ ATPases (ClpA, ClpX, and ClpB), which belong to the Clp/Hsp100 family along with Hsp104, also function by unfolding and translocating their substrates[24-26]. Furthermore, two of these (ClpA and ClpX) can couple to a protease (ClpP) to degrade their substrates after translocation. ClpA, ClpX, and ClpB have been studied extensively *in vitro* and *in vivo* and have provided insight into how this class of proteins function as molecular motors. The work described in chapter 2 aimed to develop a robust *in vitro* system to study the interactions between prions and these molecular motors.

CHAPTER 2

Interplay between strain conformation and primary structure of the yeast [*PSI*$^{+}$] prion protein

Interplay between strain conformation and primary structure of the yeast [*PSI*$^{+}$] prion protein

Katherine J. Verges[2,3], Brandon H. Toyama[2,3], Jonathan S. Weissman[1,2,3]

[1]Howard Hughes Medical Institute

[2]California Institute of Quantitative Biomedical Science

[3]Department of Cellular and Molecular Pharmacology

University of California, San Francisco, 1700 4th Street, San Francisco, CA 94158-2542, USA

Correspondence:

Jonathan S. Weissman

415-502-7642 (phone)

415-514-0273 (fax)

weissman@cmp.ucsf.edu

Abstract

Prion proteins have the surprising ability to adopt multiple different infectious strain conformations. Here we examine how a prion protein's primary structure affects its capacity to propagate specific conformations by exploiting our ability to create two distinct infectious conformations, termed Sc4 and Sc37, of the yeast [*PSI*$^{+}$] prion protein, Sup35p. PNM2, a Sup35p (G58D) point mutant identified originally for its dominant interference with prion propagation, leads to rapid, recessive loss of Sc4 while not interfering with Sc37 propagation. Paradoxically PNM2 destabilizes the amyloid core of Sc37 but does not affect the structure or chaperone-mediated division of Sc4. Robust propagation of Sc37 by PNM2 arises from compensatory effects of the mutation on the Sc37 conformation, which slow prion growth but aid prion division. In contrast, for Sc4, PNM2 interferes with prion delivery to daughter cells. Thus effective delivery of infectious particles during cell division is a critical and conformation-dependent step in the prion inheritance cycle.

Introduction

Infectious proteins, or prions, are a form of conformation-based inheritance, in which a protein aggregate to binds to and catalyzes the conversion of newly made proteins to the prion form creating stably propagating states[1]. Such conformation-based inheritance underlies a range of transmissible spongiform encephalopathies in mammals as well as heritable epigenetic states in fungi. While the various proteins responsible for these different prion states are otherwise unrelated, in most but perhaps not all cases, the prion protein misfolds into β-sheet rich amyloid-like aggregates and the self templating nature of such ordered aggregates is thought to form the basis of prion propagation[1,27-32].

A number of general features of prion inheritance arise from the templated growth of the amyloid fibers[2]. For example, species barriers, which inhibit transmission between even closely related prion proteins, originate from the inherent specificity of the templated growth of amyloid aggregates and are a common feature of prion propagation[33-36]. Similarly, the existence of different strain variants, wherein prion particles composed of the same protein exhibit various *in vivo* phenotypes, results from the ability of the prion proteins to adopt multiple, distinct self-propagating amyloid forms[4,9,37]. Strain variants appear to be a nearly universal feature of prions, as a range of different strain variants has been found for both mammalian and yeast prions[4,38-41].

A remarkable interplay exists between prion strain variants and the amino acid sequence of the prion protein, as small changes in the prion protein sequence can dramatically affect the ability of prions to adopt particular strain variants[4,10-12]. The naturally occurring methionine/valine polymorphism at position 129 of the mammalian prion protein provides a striking example of this phenomenon[42]. The Val 129 allele does

not interfere with the propagation of all prion strain variants and may even favor some, including certain iatrogenic forms of Creutzfeldt-Jakob diease[12]. However, the presence of even a single allele of Val 129 appears to be highly protective against developing new variant Creutzfeldt-Jakob disease (nvCJD)[13], which is thought to result from transmission of bovine spongiform encephalopathy (mad cow disease) to humans[5,6]. The mechanistic basis of such protective effects remains obscure.

The yeast prion [*PSI*$^+$], which results from the aggregation of the translation termination factor Sup35p, provides a powerful system for investigating how changes in primary structure lead to strain variant specific inhibition of prion propagation. In particular, a mutant of the Sup35p prion protein, which was originally identified in a screen for "Psi no more" mutants that prevented propagation of [*PSI*$^+$], shows strain variant specific effects. This mutant, termed PNM2, has a glycine to aspartate missense mutation at amino acid position 58[43]. Originally, the effect of PNM2 was described as causing dominant inhibition of prion propagation when coexpressed with wild type Sup35p[43,44]. Later studies found that PNM2 does not interfere with propagation of all [*PSI*$^+$] strain variants and may enhance propagation of certain strain variants when overexpressed[10].

A key advantage of the [*PSI*$^+$] system is the ability to create defined strain variants that can be studied both *in vivo* and *in vitro*. The prion-forming domain of Sup35p can form amyloid fibers *in vitro* which cause conversion to specific [*PSI*$^+$] states upon introduction into yeast[9,20]. Furthermore, amyloid fibers formed at 4˚C and 37˚C lead to distinct conformations, termed Sc4 and Sc37, respectively[9]. Introduction of these different prion conformations into yeast leads to readily distinguishable differences in the

resulting [*PSI*$^{+}$] state. The [*PSI*$^{+}$] yeast that result from infection with Sc4 fibers ([*PSI*$^{+}$]^{Sc4}) exhibit a strong prion phenotype, in which the large majority of Sup35p is aggregated. Alternatively, infection with Sc37 fibers gives rise to yeast ([*PSI*$^{+}$]^{Sc37}) that have a more substantial pool of soluble Sup35p and a weaker prion phenotype. These studies demonstrated that strain variants are enciphered within the conformation of the amyloid. Subsequent structural studies revealed that there is a dramatic expansion (near doubling) of the amyloid core in the Sc37 conformation relative to that found in Sc4[19,30]. The more extensive structure in Sc37 amyloid fibers increases fiber stability and decreases the rate of prion replication by the cell's chaperone system resulting in the weaker [*PSI*$^{+}$]^{Sc37} prion phenotype. The ability to probe the structural characteristics of these defined strain variant conformations *in vitro* and monitor their phenotypes *in vivo* makes [*PSI*$^{+}$] a uniquely powerful system to examine the interplay between point mutations and strain variant specific prion propagation.

Here, we used the PNM2 mutant and the well-defined prion conformations, Sc4 and Sc37, together with in-depth structural and *in vivo* analyses, to investigate how point mutations can affect prion propagation in a manner that depends on the prion strain variant.

Results

PNM2 shows strain variant specific effects on [*PSI*$^{+}$] propagation

We began by systematically characterizing the effect of the PNM2 mutation on prion propagation in [*PSI*$^{+}$]^{Sc4} and [*PSI*$^{+}$]^{Sc37} yeast. To allow for rapid exchange of alleles, we used a *Saccharomyces cerevisiae* background in which the genomic copy of *SUP35* was deleted and replaced by a copy encoded on a plasmid that contains the counter-selectable *URA3* marker. We exchanged this plasmid with one encoding wild-type Sup35p (WT) or Sup35p containing the G58D mutation (PNM2) and confirmed that the two proteins were expressed at similar levels (**Fig. 1b**). We then assessed the prion phenotype with a red/white color readout that results from nonsense suppression of the *ade1-14* reporter that contains a nonsense mutation. When Sup35p is soluble ([*psi*$^{-}$]), translation of *ade1-14* terminates prematurely resulting in accumulation of a red metabolic intermediate. When Sup35p is aggregated ([*PSI*$^{+}$]), read-through of the premature stop codon occurs resulting in functional Ade1p. Depending on the amount of soluble Sup35p present, [*PSI*$^{+}$] strain variants have varying levels of functional Ade1p and exhibit specific color phenotypes that can range from pink ([*PSI*$^{+}$]^{Sc37}) to white ([*PSI*$^{+}$]^{Sc4}). In addition, this color assay reports on the stability of prion inheritance, as when a cell in a growing colony loses [*PSI*$^{+}$], all of its progeny remain prion free and results in a red sector in the colony.

Using the defined [*PSI*$^{+}$]^{Sc4} and [*PSI*$^{+}$]^{Sc37} yeast backgrounds, we found that PNM2 has dramatic strain variant specific effects on prion propagation. When expressed as the sole copy of Sup35p, PNM2 strongly compromised propagation of [*PSI*$^{+}$]^{Sc4}, most pronouncedly observed by the continuous generation of prion-free ([*psi*$^{-}$]) states (**Fig.**

1a,c,d). This effect is similar to the originally reported description of the PNM2 phenotype[43,44], though our observations differ from those studies, as PNM2 does not strongly interfere with [*PSI*$^{+}$]^{Sc4} propagation when coexpressed with WT (**Fig. 1a**). These differences may result from differences in the genetic background of the yeast or in the strain conformation of the prion, as even among distinct strain variants that are phenotypically strong (white in color), we have observed substantial differences in the degree of structure around residue 58 (data not shown). For the remainder of our studies, we focused on analyzing effects of prion propagation when PNM2 is expressed as the sole copy of Sup35p.

In marked contrast to its dramatic effect on Sc4 propagation, PNM2 had a much weaker effect on propagation of the Sc37 strain variant, as introduction of PNM2 into [*PSI*$^{+}$]^{Sc37} yeast resulted in at most a mild darkening of the color phenotype and no discernable increase in prion loss (**Fig. 1a,d**).

In principle, the defect in stable inheritance seen in [*PSI*$^{+}$]^{Sc4} yeast could arise from the PNM2 mutation forcing an irreversible structural change that results in an amyloid conformation that is poorly propagated. Alternatively, PNM2 amyloid fibers may retain the ability to adopt the wild-type structure that encodes the information specific to the Sc4 strain variant, but interfere with propagation in a different manner. For example, the PNM2 mutation may interrupt prion propagation by affecting its ability to interact with the host chaperone machinery. To distinguish between these possibilities, we carried out a series of plasmid exchanges, in which we first replaced the WT plasmid with the PNM2 plasmid then subsequently exchanged back the WT plasmid. Reintroduction of the WT plasmid fully restored the original [*PSI*$^{+}$]^{Sc4} phenotype (**Fig.**

1e). Therefore, the PNM2 Sc4 fibers were able to retain the structural information necessary to template WT to the characteristic Sc4 amyloid conformation.

PNM2's Sc4-specific defect in [*PSI*$^{+}$] propagation was surprising as previous studies revealed that the PNM2 mutation is located in a region that is structured in the Sc37 conformation, but not in the Sc4 conformation[19]. Thus, one naively might expect that the PNM2 mutation would have preferentially interfered with propagation of the Sc37 conformation. What then can account for this dramatic and negative impact on [*PSI*$^{+}$]^{Sc4} propagation, but not on [*PSI*$^{+}$]^{Sc37}? To investigate this question, we systematically tested the parameters that affect each step in the prion replication cycle (**Fig. 2**): (1) fiber growth; (2) fiber division, of which fiber stability and ability to interact with the *in vivo* chaperone prion-replication machinery are key determinants; and (3) delivery of prion particles to daughter cells during cell division.

PNM2 decreases the growth rate of Sc37 fibers, but does not affect growth of Sc4 fibers

To determine whether changes in fiber growth rates could account for the observed phenotypic differences, we compared *in vitro* growth rates of WT and PNM2. Earlier studies had found that PNM2 fibers may have a partial growth defect, but the nature of the prion strain variants in these studies was not well defined[45]. For our studies, we used a fragment of Sup35p (SupNM; residues 1-254, containing the Q/N-rich N-terminal and highly charged middle domains of Sup35p) that is necessary and sufficient to support robust prion propagation[14,15]. In *in vitro* seeded polymerization reactions, the rate of polymerization of soluble SupNM onto the ends of preexisting amyloid fibers can

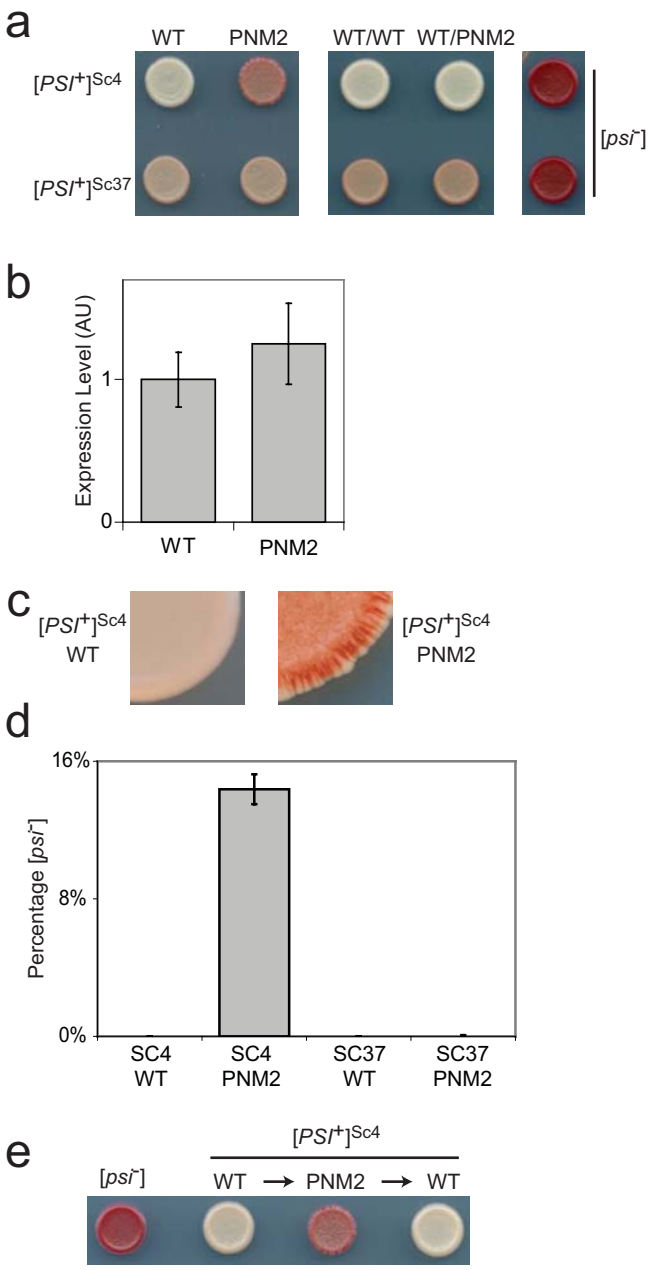

Figure 1. Characterization of *in vivo* prion phenotypes.
(a) Representative *in vivo* prion phenotypes of yeast spotted on low adenine media. WT Sup35p was replaced with either WT or PNM2 (left panel), or was coexpressed with WT or PNM2 (middle panel) in $[PSI^+]^{Sc4}$ (upper) or $[PSI^+]^{Sc37}$(lower) backgrounds. **(b)** Expression levels of WT or PNM2 expressed from a plasmid in a $[PSI^+]^{Sc4}$ background. Expression levels were quantitated by immunoblotting with a polyclonal anti-SupNM antibody. Values represent the mean ± s.d. for three experiments. **(c)** Enlarged view of the edge of the yeast spot for $[PSI^+]^{Sc4}$ WT and $[PSI^+]^{Sc4}$ PNM2. Presence of red cells indicates a loss of $[PSI^+]$. **(d)** Quantification of loss of $[PSI^+]$ as determined by counting the number of $[psi^-]$ colonies after growing for 24 hours in YEPD. Values represent the mean ± s.d. for three experiments. **(e)** Representative *in vivo* prion phenotypes of yeast spotted on low adenine media. WT Sup35p was replaced with PNM2, which was subsequently replaced with WT through plasmid exchanges.

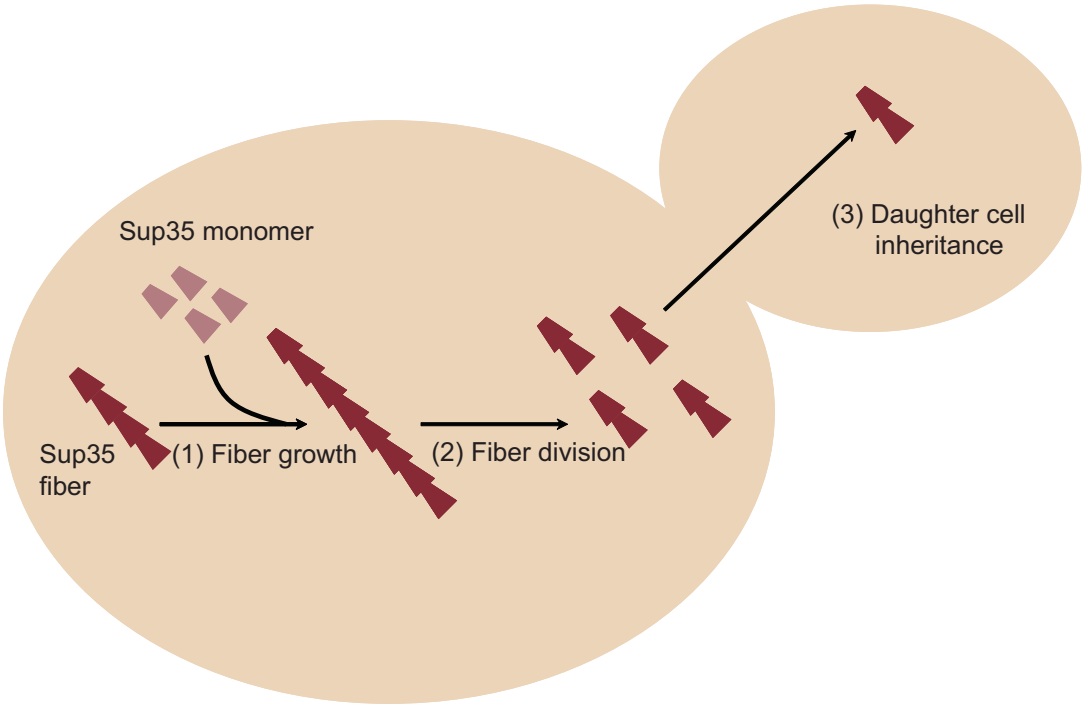

Figure 2. Schematic of the prion propagation cycle that includes (1) fiber growth, (2) chaperone mediated division, and (3) partitioning to daughter cells.

be monitored by measuring the increase in fluorescence intensity of Thioflavin T. We found that PNM2 SupNM adds onto Sc4 WT seeds at a rate similar to WT SupNM (**Fig. 3a,b**). On the other hand, we observed a decrease in the growth rate of PNM2 SupNM when polymerization was initiated with Sc37 seeds. In summary, PNM2 has an impaired growth rate only when adding onto fibers of the Sc37 conformation, in which context it showed little effect on prion propagation. Thus, the dramatic negative effect of the PNM2 mutation on $[PSI^{+}]^{Sc4}$ propagation cannot be explained by a decrease in fiber growth rate.

PNM2 affects the structure of Sc37 but not of Sc4

Differential effects on amyloid structure could in principle explain the strain variant specific effects of the PNM2 mutation, since structure and stability of a fiber would be expected to modulate prion division rates *in vivo*[18]. Accordingly, we used a range of biophysical techniques to analyze the structure and stability of PNM2 SupNM fibers in the Sc4 and Sc37 conformations. Specifically, we analyzed the structure by hydrogen-deuterium exchange NMR. These structural experiments were complemented by assessing the stabilities of the fibers by monitoring their thermal denaturation. Finally, we measured the fibers' shearing propensity, by forming long fibers in the absence of shearing forces and then subjecting them to fragmentation by stirring with a magnetic stir bar. Shearing was monitored by measuring the ability of the sheared fibers to seed monomer growth and determining the initial polymerization rates of such reactions.

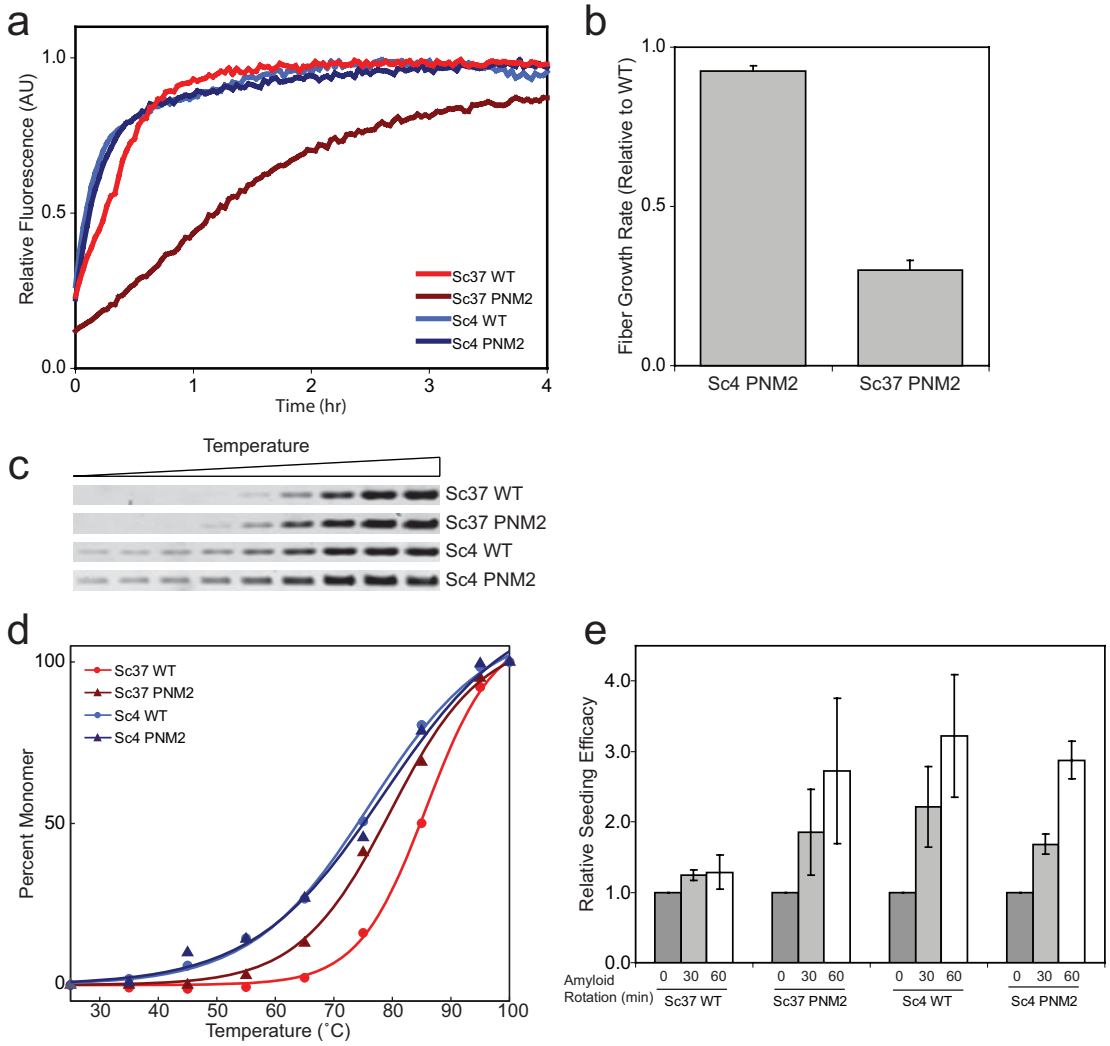

Figure 3. Characterization of the physical properties of *in vitro* formed fibers.
(a) A representative experiment monitoring the relative growth rates of WT SupNM and PNM2 SupNM. Polymerization of SupNM was performed with 5% WT seed of the specified conformation, and the rate of addition of SupNM monomers was monitored by Thioflavin T fluorescence. **(b)** The relative growth rates of WT and PNM2 SupNM. The initial growth rates of WT and PNM2 SupNM were determined by fitting the initial rate of polymerization to a line and calculating the slopes. Averages of the growth rates of PNM2 SupNM were normalized to the growth rates of WT SupNM polymerized off of the same seeds. Values represent the mean ± s.d. for three experiments. **(c,d)** Thermal stability of WT and PNM2 fibers in Sc4 and Sc37 conformations. WT and PNM2 SupNM fibers in the Sc4 or Sc37 conformations were incubated at increasing temperatures, and samples were subjected to SDS-PAGE. The band intensities, which reflect the susceptibility of aggregates to thermal solubilization, were plotted against temperature and fitted to a sigmoidal function. **(e)** Relative seeding efficacy of WT or PNM2 fibers in the Sc4 or Sc37 conformation before and after stirring for 30 or 60 min. Indicated fibers were stirred for 0, 30, or 60 minutes. After stirring, the samples were used to seed polymerization reactions, and the seeding efficacy was determined by monitoring the initial polymerization rates of these reactions. Values represent mean ± s.e.m. for three experiments.

For the hydrogen-deuterium exchange experiments, we monitored the rate of backbone amide exchange for both WT and PNM2 fibers in the Sc4 and Sc37 conformations. We looked at the extent of exchange for two different time points: after a short exchange period of 2 minutes and after a more extensive exchange period of 1 day. Based on previous assignments[19], we were able to measure the extent of exchange for 132 residues including extensive probes throughout the amyloid core of the two different conformations.

The amide exchange experiments revealed no significant differences between WT SupNM and PNM2 SupNM fibers in the Sc4 conformation (**Fig. 4a,b**). The regions of protection were similar between two samples, and the extent of protection for all residues was virtually indistinguishable. Furthermore, the extent of protection was similar for both short and long exchange times, suggesting a very strong similarity in the amyloid structure. Consistent with the above result, the melting temperatures of WT SupNM and PNM2 SupNM were comparable (77˚C ± 2 and 77˚C ± 5, respectively) (**Fig. 3c,d**). In addition, when subjected to shearing forces, both PNM2 SupNM and WT SupNM fragmented to a similar extent (**Fig. 3e**). Taken together, these results argue that PNM2 monomers are able to polymerize into fibers with an indistinguishable structure and stability to that of WT Sc4 fibers, and thus the defect in Sc4 propagation is not structural in nature.

In contrast, PNM2 induced specific localized structural defects in the Sc37 conformation. Specifically, hydrogen-deuterium exchange NMR revealed that the PNM2 mutation causes a region of increased exchange in residues proximal to the site of the PNM2 mutation (residue 58). This decreased protection is visible for both early (2 min)

and late (1 day) exchange time points (**Fig. 4c,d**). Consistent with this result, we observed a decrease in the thermal stability of PNM2 SupNM Sc37 fibers (T_m = 80˚C ± 2) compared to WT SupNM Sc37 fibers (T_m = 86˚C ± 2) (**Fig. 3c,d**). Additionally, when subjected to shearing forces, PNM2 SupNM Sc37 fibers fragmented significantly more than WT SupNM Sc37 fibers (**Fig. 3e**). These results suggest that the PNM2 mutation in the Sc37 conformation causes a localized destabilization of structure and a decrease in overall fiber stability. This localized structural defect would be expected to enhance the rate of prion division *in vivo*, increasing the rate of generation of free fiber ends and tending to strengthen the prion phenotype[18,19]. Therefore, we hypothesize that the overall effect of the PNM2 mutation on the propagation of $[PSI^+]^{Sc37}$ is the result of the compensatory effects of a slower fiber growth rate and an increased rate of fiber division.

PNM2 does not affect the ability of Sc4 fibers to interact with the chaperone machinery responsible for *in vivo* division

The above *in vitro* analysis of Sc4 amyloid fibers revealed that the PNM2 mutation does not alter the structure of the Sc4 fibers, despite negatively impacting $[PSI^+]^{Sc4}$ propagation. Since the *in vivo* division of yeast prions is carried out by chaperone machinery, we reasoned the PNM2 mutation may disrupt interactions between Sc4 prion particles and these molecular chaperones, thereby inhibiting division of prion particles *in vivo*. A growing body of evidence indicates that Hsp104, Ssa1 (Hsp70), and Sis1 (Hsp40) act in concert to sever prion particles[16,21-23]. Specifically, Ssa1 and Sis1 bind to prion particles and deliver them to Hsp104. Then, Hsp104 is thought to extract

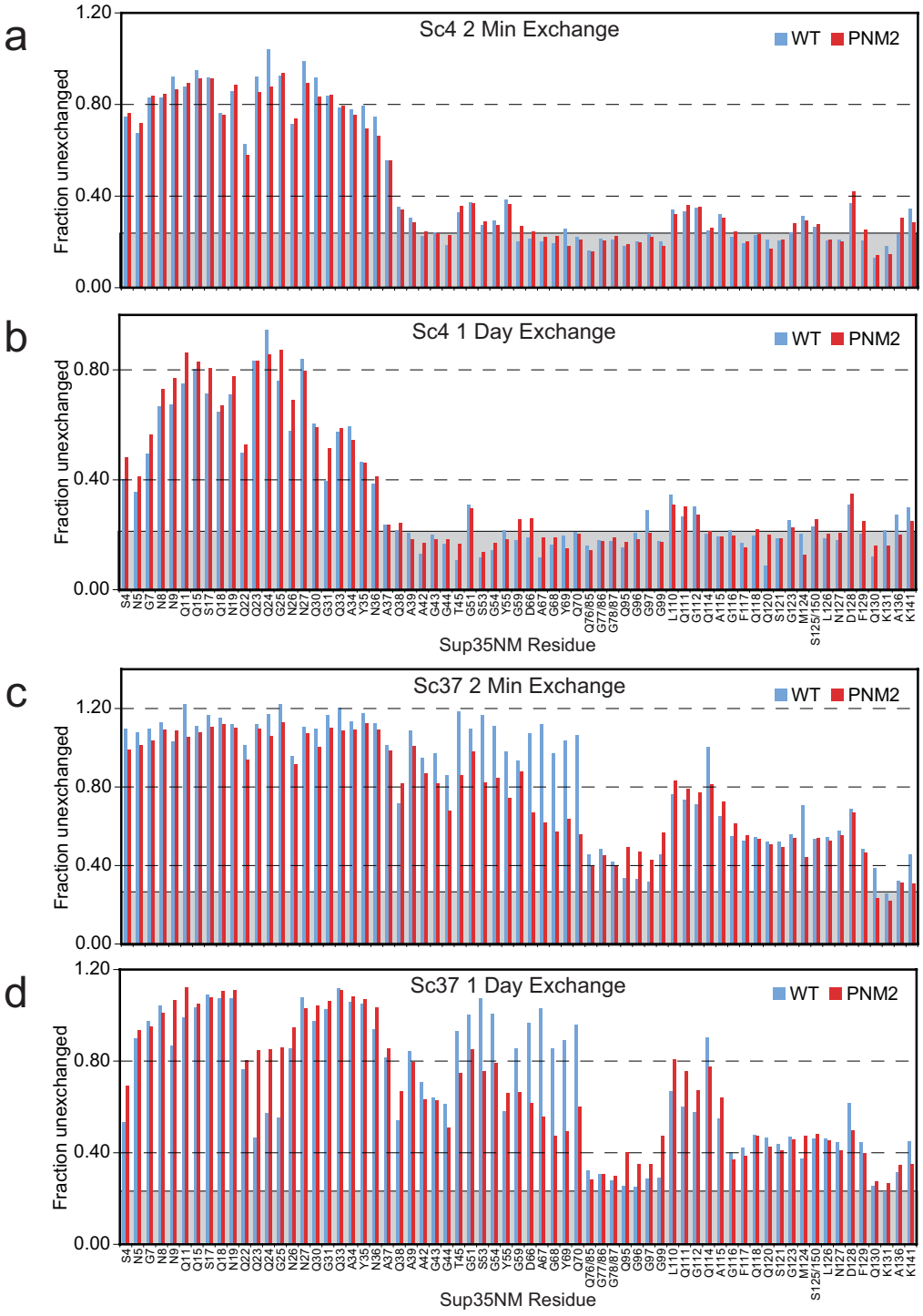

Figure 4. H/D exchange of WT and PNM2 SupNM fibers.
Intensities for assigned and unambiguous peaks corresponding to residues 1-141 were plotted as the fraction of the non-exchanged intensity after 2 min **(a, c)** and 1 day **(b, d)** of exchange for both WT (blue) and PNM2 (red) fibers in the Sc4 **(a, b)** and Sc37 **(c, d)** conformations. Unassigned and ambiguous residues are not displayed. The gray bar represents the estimated minimum peak intensity following complete exchange.

prion monomers from fibers in an ATP dependent process that involves translocation of the extracted monomers through the axial pore of Hsp104.

Recently, a system was developed for monitoring the flux of substrates through Hsp104 (**Fig. 5a**). Tessarz et al.[46] and Tipton et al.[23] engineered derivatives of Hsp104 (HAP and 4BAP, respectively) that interact with ClpP, a bacterial protein that forms a proteolytic chamber. When ClpP and HAP are coexpressed, substrates of Hsp104 are translocated into the proteolytic chamber of ClpP and degraded. When used in conjunction with a catalytically dead mutant of ClpP ($ClpP^{trap}$), this system leads to trapping of substrates. Thus, affinity purification of $ClpP^{trap}$, following its induction in a HAP-expressing yeast background, allows identification of Hsp104's substrates. Importantly, Sup35p is delivered to $ClpP^{trap}$ in a HAP-dependent manner, and the amount of trapped Sup35p depends on the prion state, as Sup35p translocates through HAP into $ClpP^{trap}$ only in [*PSI*$^+$] cells[23,46]. Moreover, significantly less Sup35p is trapped in the weak [*PSI*$^+$]^{Sc37} strain than in the strong [*PSI*$^+$]^{Sc4} strain[23], which is known to be more efficiently divided *in vivo*[18]. Since translocation is likely to be a terminal event, defects in any chaperone interactions that are required for prion division would be expected to yield a difference in the trapping efficiency of Sup35p.

First, we confirmed that WT Sup35p was trapped in a [*PSI*$^+$]-dependent manner (**Fig. 5b**). Then, we looked at the amount of trapped PNM2 when it was expressed as the sole source of Sup35p (**Fig. 5c**). Surprisingly, we found that PNM2 fluxed through Hsp104 at a similar level to WT. To investigate this further, we looked at the trapping efficiency in yeast that coexpressed HA-tagged PNM2 and untagged WT simultaneously (**Fig. 5d**). When PNM2 and WT were both present, they were both captured in the trap at

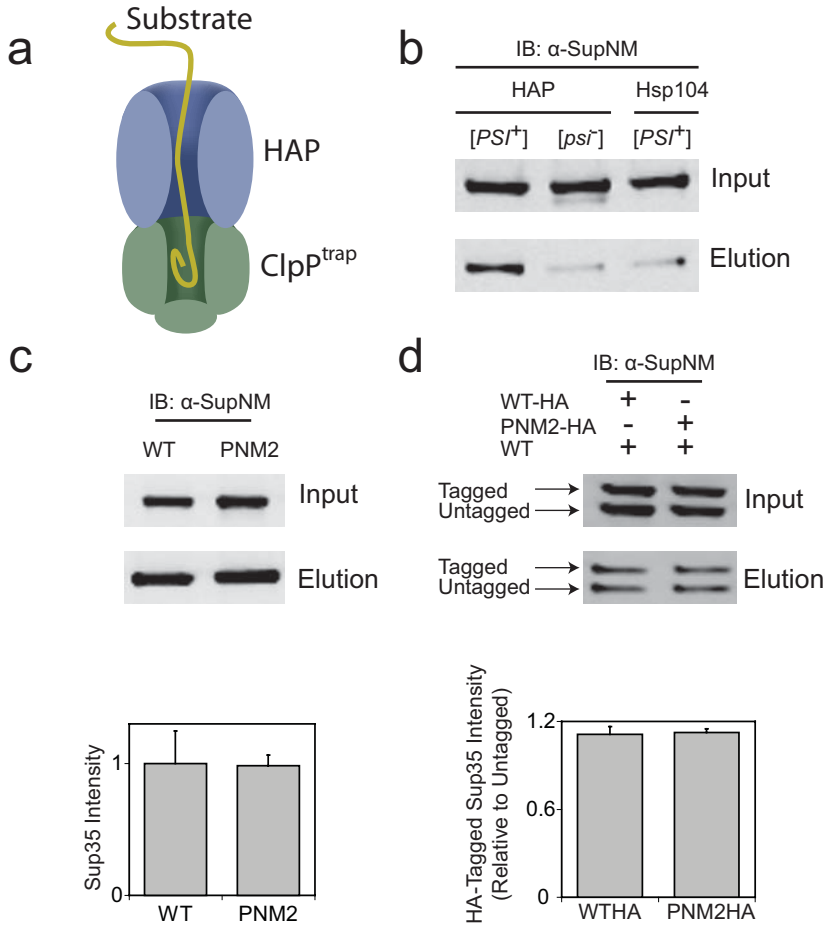

Figure 5. PNM2 fibers in the Sc4 conformation interact with the *in vivo* chaperone machinery. **(a)** Schematic of the *in vivo* HAP/ClpP^{trap} reaction. HAP, an engineered variant of Hsp104, translocates its substrates into ClpP^{trap}. ClpP^{trap} is subsequently affinity purified, and associated substrates are identified by western blotting. **(b)** Representative blot of the ClpP^{trap} affinity purification. WT Sup35p and ClpP^{trap} were expressed in backgrounds that were [*PSI*$^{+}$]^{Sc4} or [*psi*$^{-}$] expressing HAP or Hsp104p. After affinity purification of ClpP^{trap}, Sup35p was probed for by western blotting using polyclonal anti-SupNM. **(c)** Monitoring the translocation of PNM2. HAP and ClpP^{trap} were expressed in [*PSI*$^{+}$]^{Sc4} cells that also expressed WT Sup35p or PNM2. After affinity purifying ClpP^{trap}, Sup35p was probed for by western blotting (top panel). Intensities of Sup35p elution signal were normalized for input signal and averaged over 3 experiments (bottom panel). Values are expressed as mean ± s.e.m. **(d)** Monitoring translocation of PNM2 when coexpressed with WT. HAP, ClpP^{trap}, and untagged WT Sup35p were coexpressed in [*PSI*$^{+}$]^{Sc4} cells that also expressed HA-tagged WT or HA-tagged PNM2. After affinity purifying ClpP^{trap}, Sup35p was probed for by western blotting (top panel). The higher molecular weight band corresponds to HA-tagged Sup35p while the lower molecular weight band corresponds to untagged Sup35p. Intensities of tagged-Sup35p elution signals were normalized for input signal and for untagged-Sup35p elution signal and were averaged over 3 experiments (bottom panel). Values are expressed as mean ± s.e.m.

similar levels. The observed lack of effect on the trapping efficiency of PNM2 argues against a defect in Hsp104-mediated prion division being the primary cause of PNM2's inability to propagate [*PSI*$^{+}$]^{Sc4}.

PNM2 causes a defect in Sc4 propagon partitioning.

We next investigated whether the PNM2 mutation causes a defect in delivery of [*PSI*$^{+}$]^{Sc4} infectious particles (propagons) to daughter cells during cell division using a method developed by Cox, Ness, and Tuite[47]. After separation by micromanipulation, corresponding pairs of mother and daughter cells are grown on media containing guanidine HCl, which inhibits prion replication by reversibly inhibiting Hsp104[48-50]. The number of propagons is thought to remain relatively fixed as the cells divide, allowing dilution of the propagons to no more than one propagon per cell. The cells are then plated on media without guanidine, and the number of [*PSI*$^{+}$] colonies that arise from the mother versus the daughter represents the relative number of propagons in each mother/daughter pair. Although relating the number of observed colonies to the absolute number of prion particles is indirect, this assay allows one to monitor the relative number of propagons in mother versus daughter pairs and to observe complete loss of [*PSI*$^{+}$] by one of the partners.

We used the above assay to estimate the number of propagons in mother/daughter pairs for [*PSI*$^{+}$]^{Sc4} cells expressing WT Sup35p or PNM2 Sup35p (**Fig. 6a, b**). Consistent with previous results[47,51], analysis of WT [*PSI*$^{+}$]^{Sc4} cells showed a mild bias in the distribution of propagons toward the mother and a positive correlation between the number of propagons in the mother and daughter. However, for PNM2 [*PSI*$^{+}$]^{Sc4} cells, we observed no such correlation and even some daughter cells that had more propagons

than their mothers. Most strikingly, for a prominent subset of samples, the mother contained a large number of propagons while the daughter did not inherit any, indicating a loss of [*PSI*$^{+}$] in the daughter. In contrast, we did not observe any pairs in which the daughter had propagons, but the mother did not. The failure of propagons to partition into daughter cells is consistent with the observed *in vivo* phenotype that we see with [*PSI*$^{+}$]^{Sc4} PNM2 yeast, whose most pronounced characteristic is the appearance of red [*psi*$^{-}$] sectors.

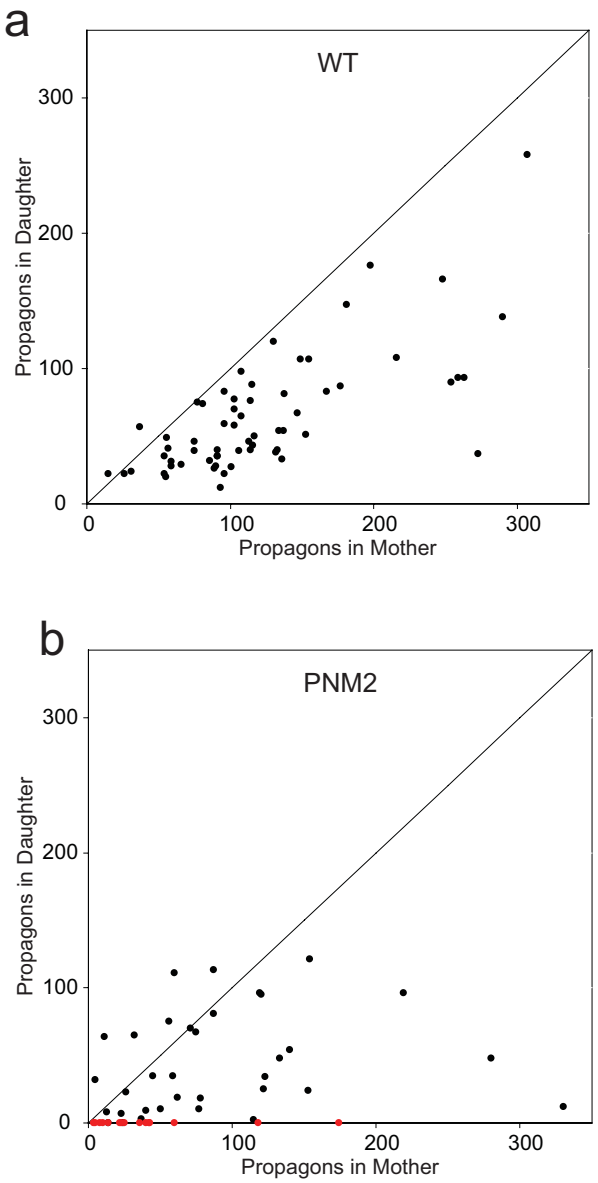

Figure 6. PNM2 in the Sc4 conformation shows a defect in partitioning.
The numbers of propagons in mothers and in daughters were determined as described in the methods section. The number of propagons in the daughter was plotted against number of propagons in the mothers for both WT **(a)** and PNM2 **(b)** [*PSI*$^{+}$]^{Sc4} backgrounds. Red dots represent mother/daughter pairs in which the mother contained propagons, but the daughter did not.

Discussion

Here, we describe the effects of a single amino acid change on the propagation of two prion strain variants. In the case of Sc37, the PNM2 mutation affects the structural and physical characteristics of the amyloid fibers, but has at best a mild effect on prion propagation *in vivo*. A different case, however, emerges from studying PNM2 in the context of Sc4, where the mutation does not affect the amyloid structure, but has a striking negative effect on propagation.

Sc37 PNM2 fibers show clear but potentially compensatory effects on fiber growth rates and stability. Although the growth of the fiber is slowed, the fibers are more fragile, allowing increased fiber division[18]. Results from the amide exchange experiment provide an explanation for these observations, as it reveals a local destabilization of the Sc37 PNM2 fibers.

The effect of PNM2 on Sc4 points to a critical role for the least understood step of [*PSI*$^+$] propagation: the partitioning of prion particles. We saw no effects on fiber growth rate, fiber structure or the ability to be acted on by the Hsp104-mediated division machinery *in vivo*. Instead, we observed a pronounced defect in the delivery of aggregates to daughter cells. These observations raise intriguing questions regarding how prions are delivered to daughter cells and what role the host machinery may play in this process. Specifically, this work highlights a central question of yeast prion biology: are [*PSI*$^+$] particles delivered to daughter cells solely through passive diffusion or by an active mechanism that ensures faithful propagation?

Past studies indicate that the observed mother bias is roughly consistent with differences in cell volume between the mother and the daughter[51]. This suggests that

passive diffusion alone could account for partitioning into daughter cells, but does not exclude the possibility that there is an active partitioning mechanism. If there is an active partitioning mechanism, then the PNM2 mutation may disrupt the interactions between the prion and the host factors responsible for their segregation. The PNM2 mutation is outside of the amyloid core of the Sc4 conformation and would in theory be accessible to interact with other cellular components.

If [*PSI*$^+$] particles do indeed reach the daughter cell by passive diffusion, the PNM2 mutation may impair the ability of Sup35p prions to escape surveillance by the cellular mechanisms that prevent damaged and aggregated proteins from entering the daughter bud. Recently, it was shown that cells collect cytosolic aggregates at defined cellular locations, presumably to minimize their negative effects on the cell's viability[52]. Furthermore, other studies have provided evidence that damaged proteins are selectively retained in the mother cell through an active mechanism[53]. However, Sup35p aggregates appear to escape both of these surveillance mechanisms, as [*PSI*$^+$] particles exist as diffuse aggregates in the cytosol when expressed at endogenous levels [54]. If [*PSI*$^+$] particles are delivered to daughter cells through unhindered passive diffusion, then remaining diffusible would be essential for stable propagation. Thus, it is possible that the PNM2 mutation prevents the ability of [*PSI*$^+$] particles to evade these protective mechanisms, leading to a defect in partitioning and the resulting sectoring phenotype.

Our studies illustrate the importance of delivery of infectious proteins to daughter cells as a critical step in the [*PSI*$^+$] propagation cycle. In the future, we anticipate that the [*PSI*$^+$] system will prove useful for studying how cells survey, partition, and sequester protein aggregates. The PNM2 mutation should provide a critical tool for such studies, as

it exhibits a distinct partitioning defect that is not confounded by changes in amyloid structure.

Acknowledgements

We would like to thank B. Bukau, A. Mogk, and P. Tessarz for reagents; M. Kelly for NMR assistance; D. Cameron, S. Collins, C. Gross, D. Mullins, G. Narlikar, M. Tanaka, and K. Tipton for helpful discussions; and O. Brandman, C. Foo, A. Frost, N. Ingolia, E. Oh, E. Quan, M. Smith, and E. Rodriguez for critical reading of the manuscript. This work was funded by the Howard Hughes Medical Institute (J.S.W.), the National Science Foundation Graduate Research Fellowship program (K.J.V), and the National Institutes of Health.

Author Contributions

KJV and JSW designed this study and wrote the manuscript. JSW supervised this work. KJV performed the majority of the experiments. BHT designed the H/X NMR experiments and acquired and analyzed the NMR data.

Materials and Methods

Strains and plasmids

Sc Strain	Description	Genotype	Source
YJW1109	74D-694 [*psi-*]	74D-694 *ade1-14 his3Δ200 leu2-3,112 trp1-289 ura3-52 sup35::TRP1*/pRS316 WT Sup35p [psi^-]	this study
YJW1110	74D-694 $[PSI^+]^{Sc4}$	74D-694 *ade1-14 his3Δ200 leu2-3,112 trp1-289 ura3-52 sup35::TRP1*/pRS316 WT Sup35p $[PSI^+]^{Sc4}$	this study
YJW1111	74D-694 $[PSI^+]^{Sc37}$	74D-694 *ade1-14 his3Δ200 leu2-3,112 trp1-289 ura3-52 sup35::TRP1*/pRS316 WT Sup35p $[PSI^+]^{Sc37}$	this study
YJW1112	W303 $[PSI^+]^{Sc4}$ HAP	W303 *ade1-14 leu2-3,112 his3-11,15 trp1-1 can1-100 ura3::nat hsp104::TRP1*/phs313HAP $[PSI^+]^{Sc4}$	this study
YJW1115	W303 $[PSI^+]^{Sc4}$ HAP	W303 *ade1-14 leu2-3,112 his3-11,15 trp1-1 can1-100 ura3::kan hsp104::*HAP_*TRP1 Sup35::nat*/pRS316 WT Sup35p $[PSI^+]^{Sc4}$	this study

All strains were converted to [PSI^+] by infection with *in vitro* formed Sc4 or Sc37 fibers as described previously[9].

Plasmid	Description	Source
pRS316 WT Sup35	pRS316; *SUP35*	this study
pRS315 WT Sup35	pRS315; *SUP35*	this study
pRS315 PNM2 Sup35	pRS315; *SUP35 G58D*	this study
phs313 Hsp104	phs313; *HSP104*	Tessarz et al.[46]
phs313 HAP	phs313; HAP	Tessarz et al.[46]
pmCUP425-ClpP^{trap}	pmCUP425; ClpP^{trap} (ClpPΔ1-13, S111A; SBP-tagged)	Tessarz et al.[46]
pRS313 WT Sup35	pRS313 *SUP35*	this study
pRS313 PNM2 Sup35	pRS313 *SUP35 G58D*	this study
pRS313WT Sup35HA	pRS313 *SUP35* with 3HA inserted after amino acid 216	this study
pRS313PNM2 Sup35HA	pRS313 *SUP35 G58D* with 3HA inserted after amino acid 216	this study

Fiber preparation

Fibers were produced as described previously, using bacterially produced pure SupNM proteins carboxy-terminally tagged with 7x-histidine[35].

***In vivo* yeast prion propagation characterization**

YJW1110 and YJW1111 were transformed with a *LEU2*-marked plasmid expressing WT or PNM2 from the endogenous promoter (pRS315 WT Sup35p or pRS315 PNM2 Sup35p, respectively). The resulting transformants were selected on media lacking uracil and leucine (SD-Ura-Leu), then subsequently passaged on YEPD, then 5-FOA, then 1/4 YEPD. For the swap back experiment, the [*PSI*$^{+}$]^{Sc4} yeast background containing the pRS315 PNM2 Sup35p plasmid was transformed with the original pRS316 WT Sup35p plasmid. Resulting transformants were selected on SD-Ura-Leu. After passaging several times on SD-Ura, colonies that required leucine for growth

were identified. The [*PSI*$^+$] phenotype was determined by observing the color on low adenine media (1/4 YEPD). The degree of sectoring, or loss of [*PSI*$^+$], was determined by growing cultures in YEPD liquid media for 24 hours at 30˚C and plating onto 1/4 YEPD plates at a density of ~400 colonies/plate. The number of [*PSI*$^+$] and [*psi*$^-$] colonies were then counted.

In vitro analysis of the physical properties of strain conformations

Fiber growth rates[19], thermal stabilities[9], and susceptibility to shearing[18] were all determined as described previously.

H/X NMR

Uniformly ^{15}N labeled SupNM was expressed in *E. coli* and purified as previously described[19]. ^{15}N-SupNM seeded fibers of each strain were made as described[19] and concentrated to 1/25th of their original volume. The fibers were then diluted 1:10 into D_2O buffer at pH 7.0 to begin the exchange. After the desired time, exchange was quenched by adjusting the pH to 2.5, and fibers were centrifuged at 100,000*g* for 25 min. The pellet was washed once with 5mM DCl in D_2O, then centrifuged again at 100,000*g* for 20 min. The pellet was frozen, freeze-dried and stored at -80˚C until NMR acquisition. The NMR spectra were acquired as described previously[19]. Estimated minimum peak intensity was calculated by averaging the intensity of a set of fully exchanged residues.

ClpP^{trap} Affinity Purification Experiments

The ClpP^{trap} affinity purification experiments were performed as described previously[46]. YJW1112 was transformed with phs313 HAP or phs313 Hsp104. The [*psi*$^-$] background was generated by transforming phs313 HAP into YJW1112 that had previously lost the pRS315 Hsp104 plasmid. YJW1115 was transformed with pRS313 WT Sup35p, pRS313 PNM2 Sup35p, pRS313 WT Sup35HA, or pRS313PNM2 Sup35HA. For experiments with yeast backgrounds containing only one copy of *SUP35*, the original pRS316 WT Sup35 plasmid was selected against by streaking onto media containing 5-FOA. All yeast cultures were grown in SD media with 50 μM $CuSO_4$ from OD_{600} = 0.1 to 1 and lysed at 4˚C by bead beating in IP buffer (50 mM Tris/Cl pH 8.0, 1 M NaCl, 2 mM EDTA, 0.5% Triton X-100, 5 mM β-mercaptoethanol, + Roche Complete Protease Inhibitor Cocktail). The lysate was cleared by centrifugation at 15,000*g* for 15 min, incubated with Streptavidin Sepharose (GE Healthcare) at RT for 1 hr, washed with 40 column volumes of IP buffer, and eluted in IP buffer + 150 mM NaCl and 4 mM biotin. The eluate was subjected to SDS PAGE and western blotting.

Mother/Daughter propagon counting

The propagons in mothers and daughters were counted as described previously[47]. Briefly, mothers and daughters of YJW1110 (containing pRS315 WT Sup35 or pRS315 PNM2 Sup35 as the sole source of Sup35) were separated by micromanipulation onto YEPD plates containing 3mM Guanidine HCl. After growing at 30˚C for about 40 hours, whole colonies were isolated using a cut pipette tip, resuspended in a small

volume of H_2O, and plated onto SD-Ade + 5% YEPD. After growing at 30˚C for 10 to 14 days, the number of [*PSI*$^+$] colonies was counted. For the WT samples, [*PSI*$^+$] colonies were easily distinguished from [*psi*-] and Ade revertants by color. The PNM2 samples contained background indistinguishable from true [*PSI*$^+$] colonies by color. We estimated the average background by repeating the experiment using a [*psi*$^-$] PNM2 strain created by curing the [*PSI*$^+$]^{Sc4} PNM2 strain by successive passaging on YEPD containing 3 mM guanidine HCl. The average background of ~25 colonies per sample was subtracted for all counted values.

CHAPTER 3

Attempt to create a self-contained prion/chaperone pair

Abstract

The AAA+ ATPase Hsp104 is thought to sever [*PSI*$^{+}$] prion particles *in vivo* through a mechanism that involves translocation of Sup35 monomers through its central pore. A detailed, mechanistic of how this process occurs, however, has not been developed. Given the structural and mechanistic similarities between Hsp104 and its homologues in *E. coli* (ClpA and ClpX) which are amenable to biochemical analyses, we attempted to create a system by which ClpA and ClpX recognize and sever Sup35 fibers. Although ClpA and ClpX could unfold and translocate SupNM monomers, they were unable to act on SupNM fibers or propagate [*PSI*$^{+}$] *in vivo*.

Introduction

Although many proteins form amyloids, only a certain subset can be propagated. The prion replication cycle involves three steps: growth, division, and distribution to daughter cells. First, fibers grow by addition of soluble monomers to preexisting seeds. Next, the fibers must be divided to form new seeds. Finally, these seeds are distributed to daughter cells during cell divisions. In order for a prion to be stably propagated, it must contain a domain that mediates growth of fibers and a domain that allows for seed formation through interaction with the chaperone machinery. With Sup35 from *S. cerevisiae* which forms fibrillar aggregates to yield the [*PSI*$^+$] prion state, a glutamine/asparagine rich tract is responsible for growth of the fiber, while oligopeptide repeats are necessary for fiber propagation[55]. Although the nature of *in vivo* seeds has not been definitively determined, *in vitro* formed fibers are able to seed monomers *in vitro* and convert [*psi*$^-$] yeast to [*PSI*$^+$] *in vivo*, both in a dose dependent way[9].

Propagation of [*PSI*$^+$] requires the yeast chaperone Hsp104. Yeast lacking Hsp104 lose [*PSI*$^+$] rapidly during cell divisions[17]. Moreover, [*PSI*$^+$] can be cured by growing cells on plates containing guanidine, a specific inhibitor of Hsp104[49]. Hsp104 has been reported to sever fibers[56], which offers an attractive hypothesis for its role in prion propagation: it severs fibers to ensure that prion seeds are distributed to both mother and daughter cells during cell divisions.

Hsp104 is a AAA+ ATPase that forms six-membered rings, disaggregates proteins after exposure to extreme stress conditions[57], and belongs to the Clp/Hsp100 family of proteins. Other members of this family, particularly ClpA, ClpX, and ClpB from *E. coli,* share similar architecture, conserved AAA domains, and an identical

oligomeric state. In *E. coli,* ClpB is the closest homologue of Hsp104 with respect to domain architecture and function. Both Hsp104 and ClpB are required for thermotolerance, in which they disaggregate heat denatured aggregates which are refolded in conjunction with Hsp70/Hsp40 or DnaK/DnaJ/GrpE, respectively[26,57]. ClpB carries out this disaggregase function by extracting monomers via its translocation activity[26,58]. Likewise, Hsp104 has been shown to translocate Sup35 in a [*PSI*$^{+}$]-dependent manner *in vivo*[23,46]. Despite these similarities in structure and function, how Hsp104 severs prion fibers is not understood at a detailed, mechanistic level.

The lack of robust *in vitro* assays using Hsp104 has complicated biochemical studies. Purifying active Hsp104 and verifying its activity have proven to be challenging. Moreover, Hsp104 may require additional factors from extracts to sever fibers[59], as reports conflict as to whether Hsp104 alone is sufficient for this activity[56,59]. Additionally, substrate recognition by Hsp104 and ClpB is not well understood. ClpA and ClpX from *E. coli*, which are more amenable to biochemical studies, offer an attractive alternative to Hsp104 and ClpB.

ClpA and ClpX are protein unfoldases that associate with the ClpP peptidase *in vivo* and function in protein degradation. These chaperones function by a mechanism in which they unfold and transolcate their substrates through the axial pores formed in the middle of the hexamers[24,25]. Additionally, both ClpA and ClpX recognize the discrete 11 amino acid SsrA tag with high affinity[60]. Attaching this tag to substrates allows for recognition and unfolding by both ClpA and ClpX[24,25]. Because ClpA and ClpX interact with ClpP and recognize the SsrA tag, straightforward assays exist for testing the activity of these chaperones (degradation of GFPssrA[24,25]) and for providing direct evidence for

substrate translocation (substrate trapping in catalytically inactive ClpP[24,25]). Additionally, both ClpA and ClpX do not require any additional chaperones to unfold their substrates, and ClpA has been shown to disaggregate heat-denatured aggregates without the help of other chaperones.

Several lines of evidence suggest that ClpA and ClpX will be sufficient for propagation of SsrA-tagged fibers. Since Sup35 amyloid fibers are sufficient to act as seeds *in vitro* and to convert yeast from [*psi*$^-$] to [*PSI*$^+$][9], fiber severing activity may be sufficient for seed formation *in vivo*. Additionally, ClpB, the closest prokaryotic homologue of Hsp104, is able to disaggregate heat denatured aggregates by extracting monomers via its translocation activity[26,58], which means that Hsp104 may sever fibers by an analogous mechanism. Moreover, ClpA has been shown to act as a disaggregase, functioning by a translocation-only mechanism without the help of additional chaperones[61]. Therefore, Hsp104 may sever fibers by extracting, unfolding, and translocating monomers, and ClpA and ClpX could replace this function. The goal of this work was originally to determine the minimal components of prion propagation by developing a prion/chaperone pair that is amenable to biochemical studies *in vitro* and that can propagate independent of host factors *in vivo*. However, we found no evidence that ClpA or ClpX could propagate [*PSI*$^+$] in the presence SsrA-tagged SupNM (NMssrA). Furthermore, NMssrA could not be extracted from fibers by ClpAP or ClpXP, even though the ssrA tag was accessible and sufficient for targeting to ClpAP and ClpXP.

Results

Neither ClpA nor ΔNClpX propagate [*PSI*$^+$] *in vivo*.

Before testing their ability to propagate [*PSI*$^+$], we first tested expression of ClpA and ClpX in yeast from the ADH1 and Met25 promoters. ClpA was expressed as expected, but ClpX was not (data not shown). We then deleted the N-terminal domain of ClpX to create ΔNClpX, and found that it was expressed from both promoters (data not shown). We then tested whether ClpA or ΔNClpX could propagate [*PSI*$^+$] in the presence of SupNM carboxy-terminally tagged with SsrA (NMssrA) expressed episomally from its endogenous promoter. We started by introducing ClpA expressed from the ADH1 promoter into a [*PSI*$^+$] yeast strain that contained a plasmid expressing Hsp104. Upon loss of the Hsp104 plasmid, [*PSI*$^+$] was lost, even in the presence of ClpA, as evidenced by its dark red color on low adenine media (**Fig. 1a**) and its inability to grow on media lacking adenine (data not shown). Similar results where seen for ClpA expressed from the Met25 promoter (even with several different concentrations of methionine) and for ΔNClpX expressed from both of these promoters (data not shown). Despite trying multiple conditions, we found no evidence that ClpA or ΔNClpX could propagate [*PSI*$^+$] in the presence of NMssrA.

ClpA does not sever Sup35NMssrA fibers *in vitro*.

To test whether ClpA could sever NMssrA fibers *in vitro*, we assayed the affect of incubating purified ClpA with *in vitro* formed NMssrA fibers. If ClpA were able to sever NMssrA fibers, then incubation with ClpA should increase the number of free fiber ends. We assayed the relative number of free fiber ends by measuring the initial rate of

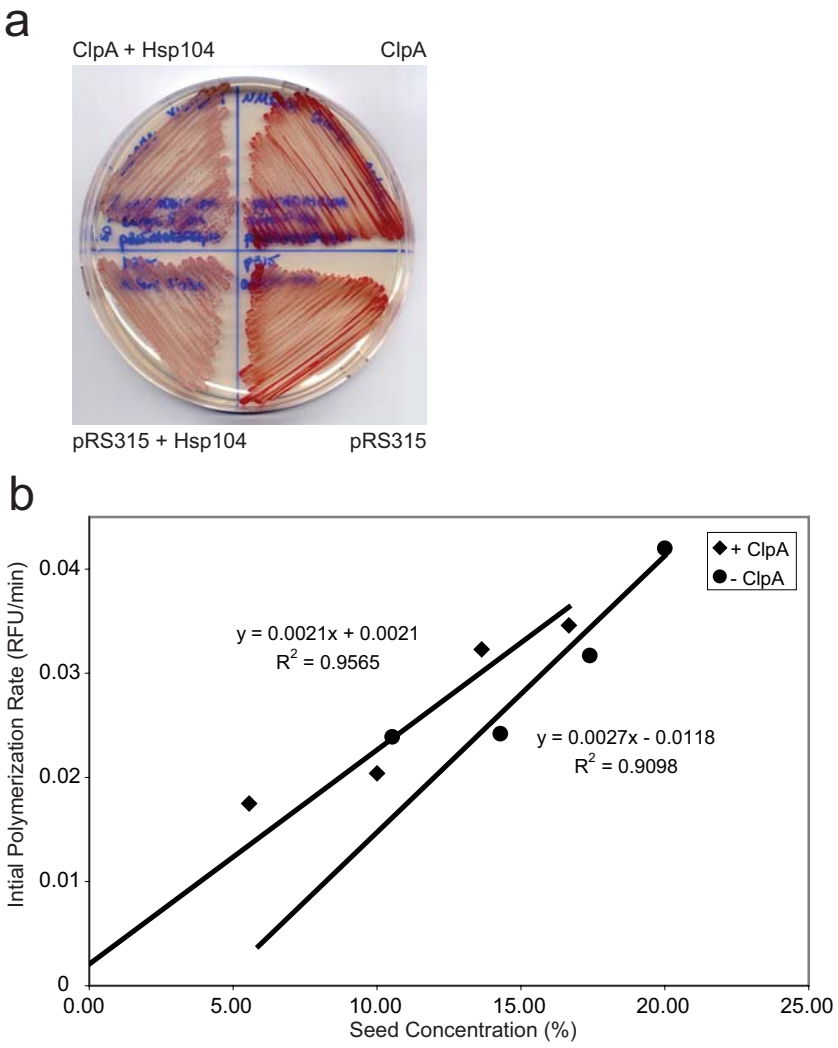

Figure 1 ClpA alone cannot propagate prions *in vivo* or sever them *in vitro*.
(a) Streaks of yeast expressing ClpA (top left), Hsp104 (bottom right), both (top left) or neither (bottom right). All strains are expressing NMssrA. [*PSI*$^{+}$] appear white to pink; [*psi*$^{-}$] appear red. **(b)** Initial rate of polymerization of SupNM off of seeds that had (diamonds) or had not (circles) been incubated with ClpA. The initial rate of polymerization correlates with the number of free fiber ends.

polymerization of SupNM monomer off of these fibers. Incubation with ClpA, however, did not increase initial polymerization rates, and therefore did not sever NMssrA fibers (**Fig. 1b**). Although it is possible that ClpA can sever fibers under different conditions, we found no evidence of such activity.

ClpA and ΔNClpX can degrade NMssrA monomers but not fibers *in vitro*.

NMssrA monomers were degraded by purified ClpAP and ΔNClpXP in vitro (**Fig. 2a,b**), albeit on a much longer time frame than the model substrate GFPssrA (data not shown). In addition to a decrease in the intensity of the NMssrA band, a lower molecular weight band increased in intensity over the course of the reaction, which may represent a degradation product. These experiments show that ClpA and ΔNClpX can recognize and act on NMssrA when monomeric.

We then tested whether ClpAP or ΔNClpXP could degrade NMssrA once polymerized into fibers. The intensity of the NMssrA band was stable over the course of the experiment (**Fig. 3a,b**), suggesting that ClpAP and ΔNClpXP did not have the capability of extracting and degrading NMssrA from fibers. Although it is possible that ClpAP and ΔNClpXP could act on different prion fibers or under different conditions, we saw no evidence to this extent.

One trivial explanation for the inability of ClpAP and ΔNClpXP to degrade NMssrA fibers is obstruction of the SsrA tag when polymerized into fibers. To test this, we determined whether NMssrA fibers could compete with GFPssrA for its degradation. In fact, NMssrA fibers did effectively compete with GFPssrA as evidenced by a slower rate of GFPssrA degradation (**Fig. 4**). Interestingly, NMssrA fibers seemed to compete

better for ClpAP and ΔNClpXP than NMssrA monomers, perhaps due to having multiple binding sites within close proximity.

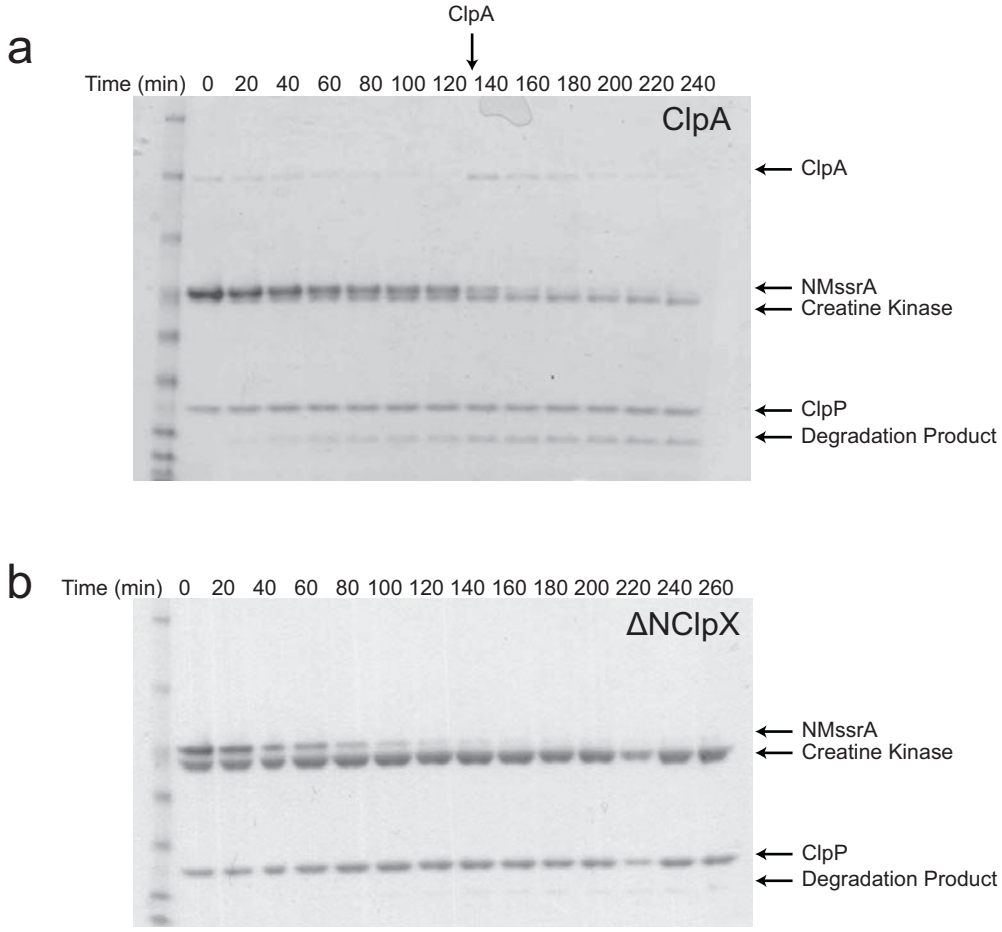

Figure 2 ClpAP and ClpXP can degrade NMssrA *in vitro*.
(a) Coomassie-stained polyacrylamide gel showing degradation of NMssrA monomers by ClpAP. Additional ClpA was added after 120 min, since ClpAP was degrading ClpA. **(b)** Coomassie-stained polyacrylamide gel showing degradation of NMssrA monomers by ClpXP.

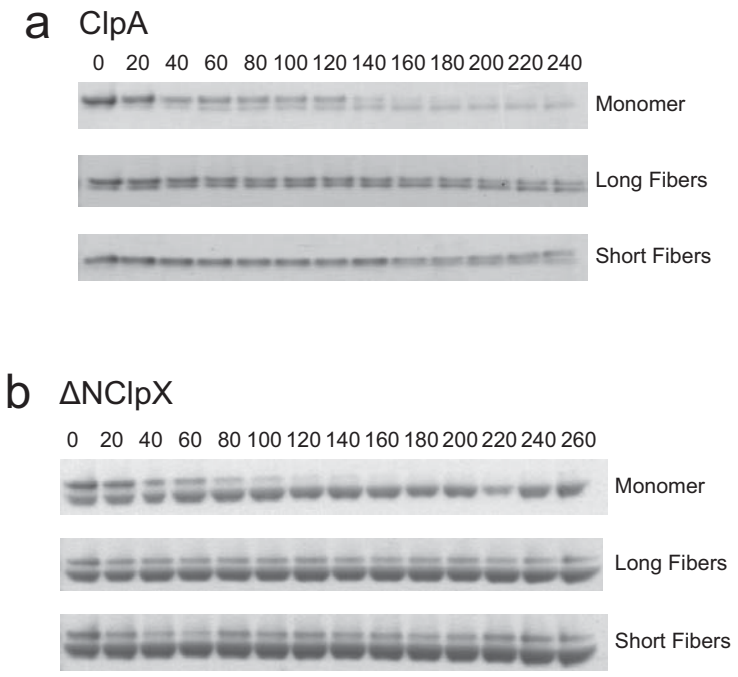

Figure 3 ClpAP and ClpXP cannot degrade NMssrA fibers.
Coomassie-stained polyacrylamide gel showing the degradation of NMssrA only when monomeric. NMssrA polymerized into fibers are stable in the presence of ClpAP **(a)** or ClpXP **(b)**.

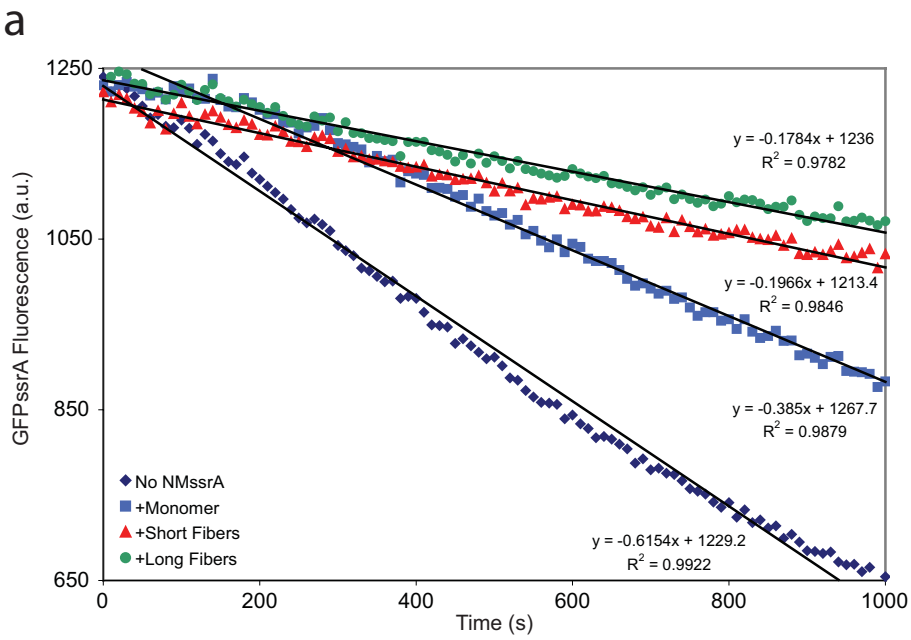

Figure 4 The ssrA tag on NMssrA is accessible to ClpAP and ClpXP.
(a) GFPssrA degradation, which was observed by monitoring the decrease in GFPssrA fluorescence over the course of the experiment, in the presence of NMssrA monomers (blue squares) or fibers (red triangles and green circles).

Discussion

The main purpose of this work was two fold: (1) to develop a robust *in vitro* system to dissect the mechanism of prion severing and (2) to create a prion/chaperone pair that could propagate independently of host factors. Unfortunately, ClpAP and ΔNClpXP do not act on NMssrA fibers, despite their recognition and ability to degrade NMssrA monomers. Thus, the orthogonal chaperone/prion system described here is not functional enough to fulfill the specified goals.

ClpAP and ClpXP are thought to work on a very wide range of SsrA-tagged substrates. Why then do they not pull NMssrA monomers out of fibers? One possibility is that the SsrA tag is poorly located. ClpA and ClpX are thought to unfold their substrates by pulling on the SsrA tag and causing a global unfolding of the adjacent domain[62]. SupNM fibers are composed of an amyloid core that spans part of the amino-terminal Q/N-rich domain, while the M-domain is highly charged and thought to be largely unstructured[19]. Since the SsrA tag is connected to the carboxy-terminus of the M-domain, it is possible that ClpA and ClpX cannot transmit their pulling force through the unstructured middle domain to extract the NMssrA monomer from the very stable amyloid core. Thus, it is possible that ClpA or ClpX could act on NMssrA fibers if the SsrA tag were located adjacent to the structured amyloid core region. Another possibility is that ClpAP and ClpXP have difficulty degrading NMssrA due to its unusual amino-acid composition. The N-domain of Sup35 is Q/N rich, which may make it problematic for ClpAP and ClpXP.

A couple of different attempts could be made to correct these potential problems. Perhaps the system would work using a different, non-Q/N rich, prion or using an internal

recognition tag. Alternatively, HAP[46] and 4BAP[23], derivatives of Hsp104 that dock to a molecular trap, provide a useful tool for developing *in vitro* or *ex vivo* biochemical assays to probe prion severing mechanisms.

Materials and Methods

Plasmids and Strains

YJW1009 was used for the *in vivo* phenotype determination experiments and has the following genotype: W303 *ade1-14 leu2-3,112 his3-11,15 trp1-1 can1-100 ura3::nat hsp104::HIS3*/pRS316*HSP104* [PSI^{+}].

Plasmid	Description	Source
pRS316Hsp104	pRS316; Heat Shock Promoter; *HSP104*	K.A. Tipton
pRS315P$_{MET25}$-ClpA	pRS315; *MET25* Promoter; ClpA; CYC1 Terminator	this study
pRS315P$_{ADH1}$-ClpA	pRS315; *ADH1* Promoter; ClpA; CYC1 Terminator	this study
pRS315P$_{MET25}$-ΔNClpX	pRS315; *MET25* Promoter; ΔNClpX; CYC1 Terminator	this study
pRS315P$_{ADH1}$-ΔNClpX	pRS315; *ADH1* Promoter; ΔNClpX; CYC1 Terminator	this study
pRS314NMssrA	pRS314; Sup35 Native Promoter; NMssrA	this study

Protein purifications

GFPssrA was a kind gift from P. Chien and T. Baker. ClpP was purified as described previously[24]. ClpA and ΔNClpX were purified using protocols from the Baker lab (see Appendix B).

Fiber preparations

Fibers were produced as described previously, using bacterially produced pure SupNM proteins carboxy-terminally tagged with 7Xhistidine[35].

In vivo phenotype determination

pRS315P$_{ADH1}$-ClpA and pRS314NMssrA were transformed into YJW1009 (which contained pRS316Hsp104) and selected on SD-leu-ura-trp. The phenotypes of the resulting transformants were determined by streaking on low adenine plates that selected for all plasmids (SD-leu-ura-trp, low ade) and on plates lacking adenine (SD-ade). These strains were struck on YEPD, then onto low adenine plates selecting the ClpA and NMssrA plasmids (SD-leu-trp, low ade) and onto plates lacking adenine (SD-ade) to assay prion phenotype. This process was repeated for all chaperone plasmids listed in above table.

ClpAP degradation assays

ClpAP degradation assays containing 250 nM ClpA$_6$, 750 nM ClpP$_{14}$, 2 μM NMssrA (monomer of fiber), 4 mM ATP, 16 mM creatine phosphate, 0.32 mg/mL creatine kinase were carried out at 30˚C in ClpA Activity buffer (25 mM Hepes-KOH, pH 7.5, 20 mM $MgCl_2$, 300 mM NaCl, 2.5% glycerol, and 0.5 mM DTT). Samples were removed from the reaction at the specified times, quenched by boiling in SDS sample buffer, and subjected to SDS-PAGE. Gels were stained with coomassie and scanned.

ClpXP degradation assays

ClpXP degradation assays containing 100 nM ClpX$_6$, 300 nM ClpP$_{14}$, 2 μM NMssrA (monomer of fiber), 4 mM ATP, 16 mM creatine phosphate, 0.32 mg/mL creatine kinase were carried out at 30˚C in PD buffer (25 mM Hepes-KOH, pH 7.6, 5 mM $MgCl_2$, 200 mM KCl, 0.032% NP-40, 10% glycerol). Samples were removed from the reaction at the

specified times, quenched by boiling in SDS sample buffer, and subjected to SDS-PAGE. Gels were stained with coomassie and scanned.

GFPssrA competition assays

GFPssrA degradation assays containing 250 nM $ClpA_6$, 750 nM $ClpP_{14}$, 2 μM GFPssrA, 0 or 2 μM NMssrA (monomer of fiber), 4 mM ATP, 16 mM creatine phosphate, 0.32 mg/mL creatine kinase were carried out at 30˚C in HO Buffer (25 mM Hepes-KOH, pH 7.5, 20 mM MgCl2, 300 mM NaCl, 10% glycerol, and 0.5 mM DTT). GFPssrA fluorescence was monitored using 467 nm excitation and 511 nm emission using a Spectramax M2 multi-detection reader with dual-mode cuvette port (Molecular Devices).

APPENDIX A

The effects of pH on fiber formation

This appendix reports observations related to the effect of pH on fiber formation. After forming SupNM fibers at 37˚C in a buffer with a pH of 6.9, I infected them into a background in which the genomic copy of *SUP35* was deleted and encoded on a plasmid. I noticed that 50% of the resulting [*PSI*$^{+}$] yeast were a color similar to what M. Tanaka had reported (conventional [*PSI*$^{+}$]^{Sc37}) (**Fig. 1b**, data not shown). The other 50% were a bright pink ([PSI^{+}]^{bright}) (**Fig. 1a**). In this text, I shall refer to them both as "strain variants" for clarity, though the bright "strain variant" may not really be a [*PSI*+] strain variant. Interestingly, the two different phenotypes always resulted in a 50%/50% ratio. Furthermore, they had different characteristics with respect to Hsp104 function and the effect of the PNM2 mutation (G58D) on their propagation (**Fig. 1c,d**). Conventional [*PSI*$^{+}$]^{Sc37} was cured by successive passaging on media containing 3 mM guanidine HCl, a specific inhibitor of Hsp104 activity. [*PSI*$^{+}$]^{bright}, however, was not cured by successive passaging on guanidine HCl. When the original WT copy of the Sup35 plasmid was exchanged for one expressing Sup35 containing the PNM2 mutation, the conventional [*PSI*$^{+}$]^{Sc37} variant was still able to propagate. PNM2, however, was not able to propagate [*PSI*$^{+}$]^{bright} variant, as [*PSI*$^{+}$]^{bright} was completely lost upon plasmid exchange.

In an effort to better understand this strange phenomenology, I looked at the fiber preparations by atomic force microscopy (AFM) (**Fig. 2a**). The fiber preparations contained fibers that had morphology similar to that which had been previously reported. These fibers were long and straight. In addition, these fiber preparations also included a second fiber type in which the fibers were curvy, and may even have been helical.

Upon testing several possible variables, I determined that the pH of the buffer best correlated with the observation of fibers with a curvy morphology (**Fig. 2b**).

Specifically, when the pH of the buffer was 7.4, almost all of the fibers within the preparation where straight by AFM and led to a conventional [*PSI*$^{+}$]^{Sc37} strain variant phenotype upon infection. When this pH was decreased to 6.9, both curvy and straight fibers were present by AFM, and both conventional [*PSI*$^{+}$]^{Sc37} and [*PSI*$^{+}$]^{bright} strain variant phenotypes were observed when infected into yeast. Even a drop of only 0.2 pH units (to pH 7.2) resulted in the presence of some curly fibers. These observations highlight the dramatic sensitivity of fiber conformation on the pH of the buffer and suggest that alternative morphologies of Sup35 fibers may exist.

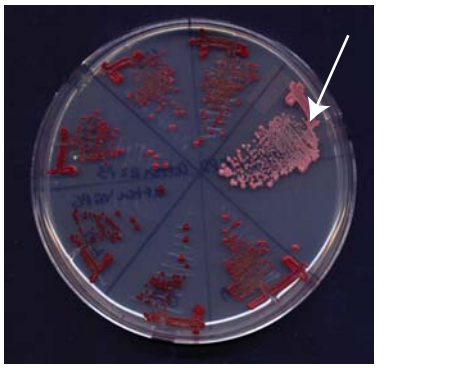

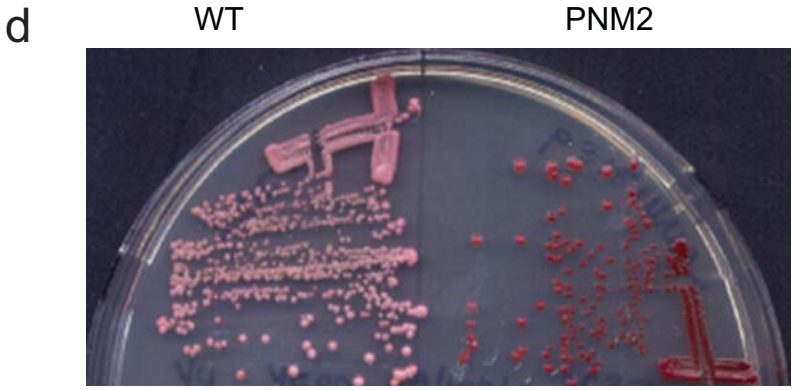

Figure 1 Description of the observed $[PSI^{+}]^{bright}$ phenotypes.
(a) Representative streak of yeast demonstrating the color of the $[PSI^{+}]^{bright}$ variant. (b) Representative streaks of M. Tanaka's documented backgrounds[9]. (c) $[PSI^{+}]^{bright}$ and conventional $[PSI^{+}]^{Sc37}$ after passaging on media containing guanidine HCl. The $[PSI^{+}]^{bright}$ sample is indicated with an arrow. (d) The effect of the PNM2 mutation on propagation of $[PSI^{+}]^{bright}$. The original WT Sup35 plasmid was replaced with one containing Sup35 with the PNM2 mutation (right).

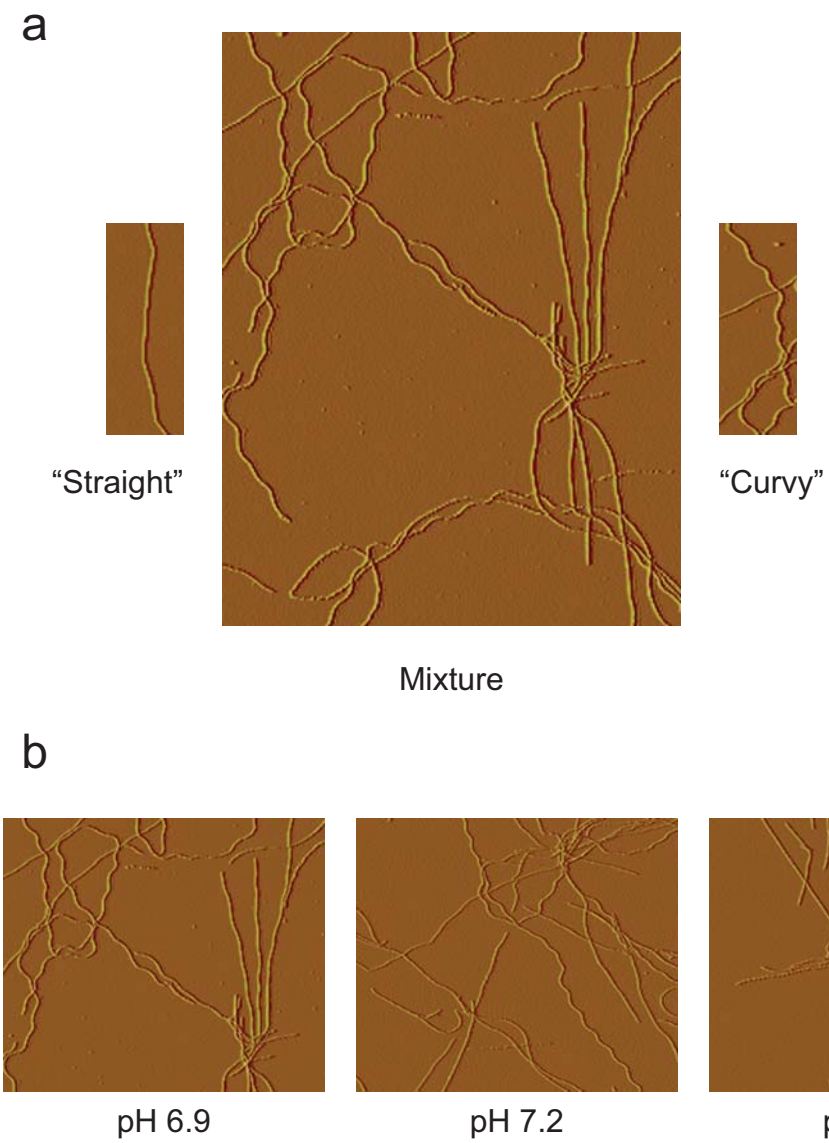

Figure 2 Morphologies of *in vitro* formed fibers.
(a) Morphologies of fibers formed in buffer with a pH of 6.9. Fibers were formed *in vitro* then imaged by AFM. A particular straight fiber (left) and a curvy fiber (right) from this mix are highlighted.
(b) Morphologies of fibers formed in buffer with a pH of 6.9 (left), 7.2 (middle), or 7.4 (right). Fibers were formed *in vitro* then imaged by AFM.

Materials and Methods

The yeast strain used was YJW1109, also known as BT8.

Genotype: 74D-694 *ade1-14 his3Δ200 leu2-3,112 trp1-289 ura3-52 sup35::TRP1*/pRS316 [*psi*$^-$]

Fibers were produced as described previously, using bacterially produced pure Sup35NM proteins carboxy-terminally tagged with 7Xhistidine[35].

[*PSI*$^+$] yeast backgrounds were generated as described previously, using a fiber infection protocol[9].

APPENDIX B

ClpA and ClpX purification protocols

ClpA Purifcation Protocol

Jon Kenniston / Julia Flynn / John Lo

General Notes

- Do all purification steps at 4°C.
- Thoroughly wash columns before use.
- All buffers should be filtered, degassed, and stored at 4°C.
- Run fractions on 8% polyacrylamide gels (ClpA = 84 kD)
- ClpA pI = 5.868 (Colibri), 6.3 (Maurizi)

Procedure

1. Grow O/N in 3 mL LB/Kan ClpA frozen stock (M169T in pET-9a, BL21(DE3)).

2. Inoculate 1 L LB/Kan each culture – 4 L total.

3. Grown until A_{600} 1.0, then induce with 0.4 mM IPTG for 2 hours.

4. Spin at 4000 rpm for 20 minutes.

5. Resuspend pellets in 5 mL Lysis Buffer.

6. Freeze overnight in -80°C.

7. Thaw cells with additional 25 mL Lysis Buffer + Calbiochem protease inhibitor cocktail.

8. French Press 2X.

9. Spin at 17,000 rpm in SS-34 rotor (15,000 rpm for SA600) for 1 hour in Sorvall. Remove and keep supernatant.

10. Slowly add crushed solid $AmSO_4$ to final concentration of 40% saturated, or add 100% saturated $AmSO_4$ to the supernatant for final concentration of 40% saturated. Incubate stirring at 4°C for 1 hour.

11. Spin at 12,000 rpm in SA-600 (20k x g) for 30 min. and resuspend pellets in enough S-column Buffer A lacking salt so that conductivity is below Buffer A (~40 mL; ~6.25 mL/g) <see step 13>.

12. Spin cloudy resuspension another 30 minutes at 12,000 rpm. Keep supernatant.

13. Check conductivity. Ensure that sample has less conductivity than S-column Buffer A alone. If needed, dilute or dialyze sample with S-Sepharose buffer without KCl, or add KCl if greatly under-conductive.

14. Run sample over S-Sepharose column (<50 mL) and elute with gradient of 0.2 M – 1 M KCl in Buffer B at 0.5-0.75 mL/min.

15. Check fractions on SDS-PAGE and compare with original over-expression sample.

16. Combine fractions and add $AmSO_4$ to be 0.6 M (~15%).

17. Run washed Phenyl-Sepharose column (10-20 mL) with Phenyl-Sepharose Buffer B with 0.6% CHAPS. Equilibrate with Buffer A.

18. Load sample onto column.

19. Gradient Buffer A to Buffer B at 2 mL/min for 60 minutes

20. Pool peak fractions and concentrate using Amicon tubes 5,000 rpm.

21. Dialyze against 4 L dialysis buffer overnight. Change 2 to 3 times.

22. Make 100 μL and 50 μL aliquots, and store at -80°C.

Buffers

Lysis Buffer:
- 50 mM Tris-Cl, pH 7.5
- 2 mM DTT
- 2 mM EDTA
- 10% glycerol

S-Sepharose Buffer A:
- 25 mM HEPES, pH 7.5
- 200 mM KCl
- 2 mM DTT
- 0.1 mM EDTA
- 10% glycerol

S-Sepharose Buffer B:
- 25 mM HEPES, pH 7.5
- 1.0 M KCl
- 2 mM DTT
- 0.1 mM EDTA
- 10% glycerol

Phenyl-Sepharose Buffer A:
- 50 mM $NaPO_4$, pH 7.5
- 2 mM DTT
- 10% glycerol
- 0.6 M $(NH_4)_2SO_4$

Phenyl-Sepharose Buffer B:
- 50 mM $NaPO_4$, pH 7.5
- 2 mM DTT
- 10% glycerol
- 0.6% CHAPS

Dialysis Buffer:
- 50 mM Tris-Cl, pH 7.5
- 100 mM KCl
- 1 mM EDTA
- 10% glycerol
- 2 mM DTT

ClpX Purification Protocol Tania Baker Lab

Note: The Baker lab specified that this protocol is faster and dirtier than another protocol that they also use. Contact them if a longer and cleaner protocol is needed.

Cell growth

ClpX can be expressed in a variety of cell types, but greater success usually results from strains that do not have "leaky" expression. Tight control of expression can usually be obtained with a BL21 pLys system but others appear to be fine as well.

Cells are grown to a high density (~A600=1.0) @ 37˚C in either LB or TB media at which point we shift the temperature to 25˚C and induce with 0.5mM IPTG shortly thereafter.

Harvested cells are resuspended in 1mL Lysis Buffer (see Buffer Recipes) per gram wet cell pellet. The paste can be stored at -80˚C until ready to purify.

Lysis/AmSO4 preciptation

1. Thaw cells, add 10mL Lysis Buffer per gram of cell pellet. Disrupt cells by either French press or gentle sonication.

2. Spin first at about 12-15k rpm (we use Sorvall RC5B with a SA600 bucket) for 1hr to generally pellet large cell debris, then additionally spin the supernate from this step in an untracentrifuge (we use a Beckman Ti45 rotor, 1 hr at 40K rpm).

3. To the supernate add ammonium sulfate to 35%**, allow to stir for at least 1 hr (but can sit overnight if needed)

4. Spin slow speed (4K RPM in Beckman J6 HC swinging bucket) to pellet AmSO4 precipitate. If you spin too fast here, step (5) is more difficult.

5. Resuspend the AmSO4 pellet with Lysis Buffer (minimize volume for a resonable load volume for the phenyl sepharose column). After allowing as much of the precipitate to resolublize (usually some material remains insoluble), spin the sample for 1 hr at 12K RPM (in the Sorvall RC5B rotor). Keep supernate.

**Note: Some purifications required that pelleting the material with 45% AmSO4 for some reason. One suggestion is to keep the supernate for the 35% cut and add additional AmSO4 to a 45% final and proceed as with the 35% cut. Check the samples at the end of step 5 for ClpX content via SDS PAGE.

Phenyl Sepharose Chromatography

1. Add ammonium sulfate to the ClpX sample until the conductivity matches the conductivity of phenyl sepharose equilibration buffer (Buffer PS-A). Obviously, too much AmSO4 at this step will precipitate the ClpX.

2. Equilibrate a HiLoad 16/10 Phenyl Sepharose High Performance column (Amersham, or similar HIC column) with buffer PS-A, load sample, and wash column with Buffer PS-A.

3. Run a gradient from 0% Buffer PS-A to 100% Buffer PS-B. ClpX generally elutes 1/2 way through the gradient.

Q-Sepharose Chromatography

1. Buffer exchange combined phenyl sepharose fractions containing ClpX into Buffer QS-A (or alternatively dilute ClpX sample to a conductivity equivalent to that of QS-A)

2. Equilibrate a HiLoad 16/10 Q Sepharose High Performance column (Amersham, or similar ion exchange resin) with Buffer QS-A, load sample, and wash column with Buffer QS-A.

3. Run gradient from 100% Buffer PS-A to 100% Buffer PS-B. ClpX generally elutes at around 300 mM KCl.

4. Pool samples, determine concentration (E280=84480 $cm^{-1}M^{-1}$), and keep frozen at -80˚C. Try to minimize number of freeze/thaws to 3-4 maximum, as some notice a loss of activity during this process.

Source 15Q Chromatography

To concentrate the ClpX sample, then run a smaller volume Source 15Q resin (Amersham) with a fast gradient and utilizing the same buffers as in the Q-sepharose column. This is preferred over spin concentrating as this causes more loss of ClpX than it concentrates.

If you are unhappy with the purification at this point, you could also try running a gel filtration column (Amersham S200) and/or a hydroxyapatite column. I'd wait to see how the above goes first though.

Buffers

Lysis Buffer:

50mM TrisCl, pH 8.0
100mM KCl
5mM MgCl2
5mM DTT
10% glycerol
Fresh 1mM PMSF

Buffer PS-A

50 mM sodium phosphate, pH 7.5
2 mM DTT
10% glycerol
0.5M (NH4)2SO4

Buffer PS-B: Buffer PS-A but no AmSO4

Buffer QS-A:

Just the Lysis Buffer w/o PMSF

Buffer QS-B: Buffer QS-A with 1M NaCl

APPENDIX C

References

1. Caughey, B., Baron, G.S., Chesebro, B. & Jeffrey, M. Getting a grip on prions: oligomers, amyloids, and pathological membrane interactions. *Annu Rev Biochem* **78**, 177-204 (2009).
2. Chien, P., Weissman, J.S. & DePace, A.H. Emerging principles of conformation-based prion inheritance. *Annu Rev Biochem* **73**, 617-56 (2004).
3. Kingsbury, S.B.P.a.D.T. Prions--infectious pathogens causing the spongiform encephalopathies. **CRC Crit Clin Neurobiol**, 181-200 (1985).
4. Morales, R., Abid, K. & Soto, C. The prion strain phenomenon: molecular basis and unprecedented features. *Biochim Biophys Acta* **1772**, 681-91 (2007).
5. Collinge, J., Sidle, K.C., Meads, J., Ironside, J. & Hill, A.F. Molecular analysis of prion strain variation and the aetiology of 'new variant' CJD. *Nature* **383**, 685-90 (1996).
6. Hill, A.F. et al. The same prion strain causes vCJD and BSE. *Nature* **389**, 448-50, 526 (1997).
7. Aguzzi, A., Sigurdson, C. & Heikenwaelder, M. Molecular mechanisms of prion pathogenesis. *Annu Rev Pathol* **3**, 11-40 (2008).
8. Bruce, M.E. TSE strain variation. *Br Med Bull* **66**, 99-108 (2003).
9. Tanaka, M., Chien, P., Naber, N., Cooke, R. & Weissman, J.S. Conformational variations in an infectious protein determine prion strain differences. *Nature* **428**, 323-8 (2004).
10. Derkatch, I.L., Bradley, M.E., Zhou, P. & Liebman, S.W. The PNM2 mutation in the prion protein domain of SUP35 has distinct effects on different variants of the [PSI+] prion in yeast. *Curr Genet* **35**, 59-67 (1999).
11. Green, K.M. et al. The elk PRNP codon 132 polymorphism controls cervid and scrapie prion propagation. *J Gen Virol* **89**, 598-608 (2008).
12. Takemura, K., Kahdre, M., Joseph, D., Yousef, A. & Sreevatsan, S. An overview of transmissible spongiform encephalopathies. *Anim Health Res Rev* **5**, 103-24 (2004).
13. Mead, S. et al. Creutzfeldt-Jakob disease, prion protein gene codon 129VV, and a novel PrPSc type in a young British woman. *Arch Neurol* **64**, 1780-4 (2007).
14. Glover, J.R. et al. Self-seeded fibers formed by Sup35, the protein determinant of [PSI+], a heritable prion-like factor of S. cerevisiae. *Cell* **89**, 811-9 (1997).
15. King, C.Y. et al. Prion-inducing domain 2-114 of yeast Sup35 protein transforms in vitro into amyloid-like filaments. *Proc Natl Acad Sci U S A* **94**, 6618-22 (1997).
16. Jones, G.W. & Tuite, M.F. Chaperoning prions: the cellular machinery for propagating an infectious protein? *Bioessays* **27**, 823-32 (2005).
17. Chernoff, Y.O., Lindquist, S.L., Ono, B., Inge-Vechtomov, S.G. & Liebman, S.W. Role of the chaperone protein Hsp104 in propagation of the yeast prion-like factor [psi+]. *Science* **268**, 880-4 (1995).
18. Tanaka, M., Collins, S.R., Toyama, B.H. & Weissman, J.S. The physical basis of how prion conformations determine strain phenotypes. *Nature* **442**, 585-9 (2006).
19. Toyama, B.H., Kelly, M.J., Gross, J.D. & Weissman, J.S. The structural basis of yeast prion strain variants. *Nature* **449**, 233-7 (2007).

20. Sparrer, H.E., Santoso, A., Szoka, F.C., Jr. & Weissman, J.S. Evidence for the prion hypothesis: induction of the yeast [PSI+] factor by in vitro- converted Sup35 protein. *Science* **289**, 595-9 (2000).
21. Higurashi, T., Hines, J.K., Sahi, C., Aron, R. & Craig, E.A. Specificity of the J-protein Sis1 in the propagation of 3 yeast prions. *Proc Natl Acad Sci U S A* **105**, 16596-601 (2008).
22. Shorter, J. & Lindquist, S. Hsp104, Hsp70 and Hsp40 interplay regulates formation, growth and elimination of Sup35 prions. *Embo J* **27**, 2712-24 (2008).
23. Tipton, K.A., Verges, K.J. & Weissman, J.S. In vivo monitoring of the prion replication cycle reveals a critical role for Sis1 in delivering substrates to Hsp104. *Mol Cell* **32**, 584-91 (2008).
24. Kim, Y.I., Burton, R.E., Burton, B.M., Sauer, R.T. & Baker, T.A. Dynamics of substrate denaturation and translocation by the ClpXP degradation machine. *Mol Cell* **5**, 639-48 (2000).
25. Weber-Ban, E.U., Reid, B.G., Miranker, A.D. & Horwich, A.L. Global unfolding of a substrate protein by the Hsp100 chaperone ClpA. *Nature* **401**, 90-3 (1999).
26. Weibezahn, J. et al. Thermotolerance requires refolding of aggregated proteins by substrate translocation through the central pore of ClpB. *Cell* **119**, 653-65 (2004).
27. Bousset, L., Thomson, N.H., Radford, S.E. & Melki, R. The yeast prion Ure2p retains its native alpha-helical conformation upon assembly into protein fibrils in vitro. *Embo J* **21**, 2903-11 (2002).
28. Dos Reis, S. et al. The HET-s prion protein of the filamentous fungus Podospora anserina aggregates in vitro into amyloid-like fibrils. *J Biol Chem* **277**, 5703-6 (2002).
29. Taylor, K.L., Cheng, N., Williams, R.W., Steven, A.C. & Wickner, R.B. Prion domain initiation of amyloid formation in vitro from native Ure2p. *Science* **283**, 1339-43 (1999).
30. Tessier, P.M. & Lindquist, S. Unraveling infectious structures, strain variants and species barriers for the yeast prion [PSI+]. *Nat Struct Mol Biol* **16**, 598-605 (2009).
31. Patel, B.K. & Liebman, S.W. "Prion-proof" for [PIN+]: infection with in vitro-made amyloid aggregates of Rnq1p-(132-405) induces [PIN+]. *J Mol Biol* **365**, 773-82 (2007).
32. Wickner, R.B., Dyda, F. & Tycko, R. Amyloid of Rnq1p, the basis of the [PIN+] prion, has a parallel in-register beta-sheet structure. *Proc Natl Acad Sci U S A* **105**, 2403-8 (2008).
33. Kocisko, D.A. et al. Species specificity in the cell-free conversion of prion protein to protease-resistant forms: a model for the scrapie species barrier. *Proc Natl Acad Sci U S A* **92**, 3923-7 (1995).
34. Santoso, A., Chien, P., Osherovich, L.Z. & Weissman, J.S. Molecular basis of a yeast prion species barrier. *Cell* **100**, 277-88 (2000).
35. Tanaka, M., Chien, P., Yonekura, K. & Weissman, J.S. Mechanism of cross-species prion transmission: an infectious conformation compatible with two highly divergent yeast prion proteins. *Cell* **121**, 49-62 (2005).
36. Vanik, D.L., Surewicz, K.A. & Surewicz, W.K. Molecular basis of barriers for interspecies transmissibility of mammalian prions. *Mol Cell* **14**, 139-45 (2004).

37. King, C.Y. & Diaz-Avalos, R. Protein-only transmission of three yeast prion strains. *Nature* **428**, 319-23 (2004).
38. Bradley, M.E., Edskes, H.K., Hong, J.Y., Wickner, R.B. & Liebman, S.W. Interactions among prions and prion "strains" in yeast. *Proc Natl Acad Sci U S A* **99 Suppl 4**, 16392-9 (2002).
39. Derkatch, I.L., Chernoff, Y.O., Kushnirov, V.V., Inge-Vechtomov, S.G. & Liebman, S.W. Genesis and variability of [PSI] prion factors in Saccharomyces cerevisiae. *Genetics* **144**, 1375-86 (1996).
40. Edskes, H.K., McCann, L.M., Hebert, A.M. & Wickner, R.B. Prion variants and species barriers among Saccharomyces Ure2 proteins. *Genetics* **181**, 1159-67 (2009).
41. Schlumpberger, M., Prusiner, S.B. & Herskowitz, I. Induction of distinct [URE3] yeast prion strains. *Mol Cell Biol* **21**, 7035-46 (2001).
42. Zeidler, M., Stewart, G., Cousens, S.N., Estibeiro, K. & Will, R.G. Codon 129 genotype and new variant CJD. *Lancet* **350**, 668 (1997).
43. Doel, S.M., McCready, S.J., Nierras, C.R. & Cox, B.S. The dominant PNM2-mutation which eliminates the psi factor of Saccharomyces cerevisiae is the result of a missense mutation in the SUP35 gene. *Genetics* **137**, 659-70 (1994).
44. Young, C.S.H., Cox, B.S. Extrachromosomal elements in a super-suppression system of yeast: I. A nuclear gene controlling the inheritance of the extrachromosomal elements. *Heredity* **26**, 413-422 (1971).
45. Kochneva-Pervukhova, N.V. et al. Mechanism of inhibition of Psi+ prion determinant propagation by a mutation of the N-terminus of the yeast Sup35 protein. *Embo J* **17**, 5805-10 (1998).
46. Tessarz, P., Mogk, A. & Bukau, B. Substrate threading through the central pore of the Hsp104 chaperone as a common mechanism for protein disaggregation and prion propagation. *Mol Microbiol* **68**, 87-97 (2008).
47. Cox, B., Ness, F. & Tuite, M. Analysis of the generation and segregation of propagons: entities that propagate the [PSI+] prion in yeast. *Genetics* **165**, 23-33 (2003).
48. Ferreira, P.C., Ness, F., Edwards, S.R., Cox, B.S. & Tuite, M.F. The elimination of the yeast [PSI+] prion by guanidine hydrochloride is the result of Hsp104 inactivation. *Mol Microbiol* **40**, 1357-69 (2001).
49. Grimminger, V., Richter, K., Imhof, A., Buchner, J. & Walter, S. The prion curing agent guanidinium chloride specifically inhibits ATP hydrolysis by Hsp104. *J Biol Chem* **279**, 7378-83 (2004).
50. Jung, G. & Masison, D.C. Guanidine hydrochloride inhibits Hsp104 activity in vivo: a possible explanation for its effect in curing yeast prions. *Curr Microbiol* **43**, 7-10 (2001).
51. Byrne, L.J. et al. The number and transmission of [PSI] prion seeds (Propagons) in the yeast Saccharomyces cerevisiae. *PLoS ONE* **4**, e4670 (2009).
52. Kaganovich, D., Kopito, R. & Frydman, J. Misfolded proteins partition between two distinct quality control compartments. *Nature* **454**, 1088-95 (2008).
53. Erjavec, N., Larsson, L., Grantham, J. & Nystrom, T. Accelerated aging and failure to segregate damaged proteins in Sir2 mutants can be suppressed by

overproducing the protein aggregation-remodeling factor Hsp104p. *Genes Dev* **21**, 2410-21 (2007).
54. Kawai-Noma, S. et al. Dynamics of yeast prion aggregates in single living cells. *Genes Cells* **11**, 1085-96 (2006).
55. Osherovich, L.Z., Cox, B.S., Tuite, M.F. & Weissman, J.S. Dissection and design of yeast prions. *PLoS Biol* **2**, E86 (2004).
56. Shorter, J. & Lindquist, S. Hsp104 catalyzes formation and elimination of self-replicating Sup35 prion conformers. *Science* **304**, 1793-7 (2004).
57. Glover, J.R. & Lindquist, S. Hsp104, Hsp70, and Hsp40: a novel chaperone system that rescues previously aggregated proteins. *Cell* **94**, 73-82 (1998).
58. Schlieker, C., Tews, I., Bukau, B. & Mogk, A. Solubilization of aggregated proteins by ClpB/DnaK relies on the continuous extraction of unfolded polypeptides. *FEBS Lett* **578**, 351-6 (2004).
59. Inoue, Y., Taguchi, H., Kishimoto, A. & Yoshida, M. Hsp104 binds to yeast Sup35 prion fiber but needs other factor(s) to sever it. *J Biol Chem* **279**, 52319-23 (2004).
60. Flynn, J.M. et al. Overlapping recognition determinants within the ssrA degradation tag allow modulation of proteolysis. *Proc Natl Acad Sci U S A* **98**, 10584-9 (2001).
61. Dougan, D.A., Reid, B.G., Horwich, A.L. & Bukau, B. ClpS, a substrate modulator of the ClpAP machine. *Mol Cell* **9**, 673-83 (2002).
62. Kenniston, J.A., Baker, T.A. & Sauer, R.T. Partitioning between unfolding and release of native domains during ClpXP degradation determines substrate selectivity and partial processing. *Proc Natl Acad Sci U S A* **102**, 1390-5 (2005).

Publishing Agreement

It is the policy of the University to encourage the distribution of all theses, dissertations, and manuscripts. Copies of all UCSF theses, dissertations, and manuscripts will be routed to the library via the Graduate Division. The library will make all theses, dissertations, and manuscripts accessible to the public and will preserve these to the best of their abilities, in perpetuity.

Please sign the following statement:

I hereby grant permission to the Graduate Division of the University of California, San Francisco to release copies of my thesis, dissertation, or manuscript to the Campus Library to provide access and preservation, in whole or in part, in perpetuity.

Katherine J Verges
Author Signature

09/02/09
Date